BIOCHEMICAL AND PROTEOMIC ANALYSES OF NORMAL HUMAN ASTROCYTES AND GLIOBLASTOMA

by

Firdevs Cansu Atılgan

Submitted to Graduate School of Natural and Applied Sciences
in Partial Fulfillment of the Requirements
for the Degree of Master of Science in
Biotechnology

Yeditepe University
2017

BIOCHEMICAL AND PROTEOMIC ANALYSES OF NORMAL HUMAN ASTROCYTES AND GLIOBLASTOMA

APPROVED BY:

Assist. Prof. Dr. Hüseyin Çimen ……
(Thesis Supervisor)

Prof. Dr. Mustafa Çulha ……

Assist. Prof. Dr. Gürler Akpınar ……

DATE OF APPROVAL: ..../..../2017

ACKNOWLEDGEMENTS

First of all, I would like to thank to my supervisor Assist. Prof. Dr. Hüseyin ÇİMEN for his support, encouragement and giving a chance to be part of his team throughout my master period. He helped me in every trouble during experimental and writing phase of my thesis.

Furthermore, I am deeply grateful to Prof. Dr. Mustafa ÇULHA for his permission to use his laboratory and I would like to thank Assoc. Prof. Dr. Dilek TELCİ for her permission to use her lab facilities.

I am so thankful my research group Eray ESENDİR, İlker KANBAĞLI and İrem BAYGUTALP and undergrad students Busem IĞNAK, İrem SOYHAN, Ayşe Tuğçe ŞAHİN, Fatih AYGENLİ, Gülşah Şebnem ÖZKÖSE and Cansu DİLEGE for their understanding and assisting during my thesis. I wish to express my thanks to İnci KURT, Gizem UÇANKUŞ and Hazel ERKAN for their endless support and patience during my master period.

I wish to express my special thanks to Çağatay Bahri AYDIN for not only his endless support, patience and love, but also for his deep understanding and encouraging me during my all master period.

Lastly but most importantly, I owe my loving thanks to my parents Huriye ATILGAN and Ahmet Duran ATILGAN for their endless encouragement, patience and unconditional love. Without their encouragement and understanding it would have been impossible for me to finish this work.

ABSTRACT

BIOCHEMICAL AND PROTEOMIC ANALYSES OF NORMAL HUMAN ASTROCYTES AND GLIOBLASTOMA

Glioblastoma is the most malignant type of brain tumor that has limited lifespan with current treatments. Cellular energy metabolism is one of the main factor which is affected during transition of a normal cell to a cancer cell. Cancer cells promote a metabolic switch for supporting their needs of biomacromolecules which are essentials for rapid growth and proliferations. Dichloroacetate in an anaolog of acetic acid and and antiglycolytic agent that is used for mitochondria disorder in medicine. In this study, we aimed to reveal the energy metabolism differences between normal human astrocytes and glioblastoma multiforme cells, and also dichloroacetate treatment to manipulate mitochondrial activity. First, glycolytic enzymes were compared between normal and glioblastoma cells upon biochemical analyses which revealed that the level of glycolytic enzymes and metabolites was elevated in cancer cells. Then mitochondrial assays were performed to determine the alterations in the mitochondrial activities of normal astrocytes and glioblastoma cells. Lastly, mass spectrometry based proteomic analysis was performed for demonstrating protein-based alterations which revealed the candidate proteins that participate in different pathways in the cell metabolism. This study, might provide a basis for metabolic differences based new approaches for cancer studies.

ÖZET

SAĞLIKLI ASTROSİT VE GLİOBLASTOMALARIN BİYOKİMYASAL VE PROTEOMİK ANALİZLERİ

Glioblastoma beyin tümörleri içinde en sık rastlanan ve ölümcül özellikte olanıdır. Günümüz tedavi koşullarıyla tedavisi en zor ve yaiam ömrü en az olan beyin kanseri türüdür. Hücre metabolizması, normal hücrenin kanserli hücreye dönüşüm aşamasında en çok etki gören ve değişim gösteren bir faktördür. Kanserleşen hücreler, hızlı büyüme ve çoğalma hızlarını karşılamak için gerekli biyomakromolekülleri hücre içi metabolizmasında kapasite arttıran değişiklikler yaparak karşılarlar. Asetik asit analoğu olan dikloroasetat, mitokondriyal bozuklukların tedavisi amacıla tıpta kullanılmaktadır. Bu çalımayla, sağlıklı astrositler ve glioblastoma kanserli hücrelerin hücre metabolizmalarında gerçekleşen değişimlerin araştırılması, dikloroasetat uygulamasıyla mitokondri metabolizmasına yapılan etkinin sonuçlarını ortaya koyulması amaçlanmıştır. İlk olarak, glikoliz metabolizmasında görevli enzim ve metabolitlerin değişimi incelenmiş ve kanserli hücrelerde artışları tespit edilmiştir. Daha sonra yapılan mitokondriyal analizlerde, mitokondri miktar ve aktivitesi kıyaslanarak, kanser hücrelerinin enerji üretiminde arttırıma gittiği gözlenmiştir. Son olarak kütle spektrometrisi analizi ile de, proteomik düzeyde oluşan farklılıklar incelenerek aday proteinler oluşturulmuştur. Bu çalışma, hücre metabolizmasındaki farkların temek alınarak gerçekleştireceği yeni yaklaşımlara öncülük edebilir.

TABLE OF CONTENTS

LIST OF FIGURES

LIST OF TABLES

LIST OF SYMBOLS/ABBREVIATIONS

2-DG	2-deoxy-D-glucose
3-BrPa	3-bromopyruvate
ACL	ATP citrate lyase
ATP	Adenosine triphosphate
BBB	Blood brain barrier
BCA	Bicinchoninic acid
BSA	Bovine serum albumin
DCA	Dichloroacetate
DCFDA	2',7' –dichlorofluorescin diacetate
ETC	Electron transport chain
FBP	Fructose-2,6-biphosphate
F6P	Fructose-6-phosphate
FADH	Flavin adenine dinucleotide
FAS	Fatty acid synthase
FBS	Fetal bovine serum
G6P	Glucose-6-phosphate
G6PD	Glucose-6-phosphate dehydrogenase
GAPDH	Glyceraldehyde-3-phosphate dehydrogenase
GBM	Glioblastoma
GLS	Glutaminase
GLUT	Glucose transporter
Hif-1α	Hypoxia inducible factor-1α
HK	Hexokinase
HSP60	Heat shock protein 60
HSP90	Heat shock protein 90
ICAT	Isotope-coded affinity tags
IDH	Isocitrate dehydrogenase
iTRAQ	Isobare tags for relative and absolute quantification
LC	Liquid chromatography
LDH	Lactate dehydrogenase

MCT	Monocarboxylate transporter
MS	Mass spectrometry
NAD^+	Nicotinamide adenine dinucleotide
NHA	Normal human astrocytes
PDC	Pyruvate deydrogenase complex
PDH	Pyruvate dehydrogenase
PDK	Pyruvate dehydrogenase kinase
PEP	Phosphoenolpyruvate
PFK	Phosphofructokinase
PFK	Phosphofructokinase
PGAM	Phosphoglycerate mutase
PGC-1α	Peroxisome proliferator-activated receptor gamma co-activator-1 alpha
PK	Pyruvate kinase
PPP	Pentose phosphate pathway
PVDF	Polyvinylidene difluoride
R5P	Ribose-5-phosphate
ROS	Reactive oxygen species
SILAC	Stable isotope labeling with amino acids in cell culture
TCA	Tricarboxylic acid
VEGF	Vascular endothelial growth factor
WHO	World health organization
α-KG	α-ketoglutarate

1. INTRODUCTION

1.1. BRAIN GLUCOSE METABOLISM

Human brain contains two per cent of all body weight; however, it consumes 20 percent of glucose-derived energy of body, which is demonstrated as ~5.6 mg glucose per 100 g human brain tissue per minute [1,2]. Glucose metabolism-derived ATP is used for maintaining the physiological function of the brain. Most of the energy consumption is related with neurons. Glucose is transported through blood-brain barrier (BBB), which is permeable for glucose but not for neuroactive compounds such as glutamate, aspartate, and glycine. Therefore, they must be synthesized in the brain [2]. Glucose transportation from blood to brain is provided via facilitative transport by glucose transporters (GLUTs). GLUT-1 is responsible for glucose uptake into the glial cell and GLUT-3 for glucose uptake into the neurons, which has higher rate of transportation [3].

During brain activation, glycolysis rate is enhanced compared to oxygen consumption rate, even if the oxygen is at sufficient level. Upregulation in glycolysis increases the release of lactate which has important roles in maintaining the functions of brain such as oxidative fuel for astrocytes and neurons, blood flow regulation, and redox signaling modulation [4]. Astrocytes are buffering neurons by being a part of BBB, provide an energy reserve by glycogen storage. They also uptake glutamate released from neurons as a part of neurotransmitter recycling and convert into glutamine via α-ketoglutarate (α-KG) synthesis for maintaining the neuronal metabolic demand. Thus, astrocytes have anaerobic glycolysis profile, but neurons have high levels of aerobic mitochondrial metabolism to meet their high energy needs in the brain [5].

1.2. BRAIN TUMORS

Brain tumors include 1.4 per cent of all cancer types and 2.3 per cent of all cancer-caused deaths. According to World Health Organization (WHO) GLOBOCAN 2012 data, in 2020 300,379 people are estimated to get brain and nervous system cancers and 225,939 people will die because of these cancers over the world. In Turkey, 5,391 people are estimated to

get brain and nervous system cancers and 3,380 people will die because of the same cancers [6]. These are classified by the histology and location of the tumor. Glioma arises from glial cells of the brain that are essential for neuron activity. Glial cells structurally support the neurons and maintain the signaling ability. Astrocytes, oligodendrocytes, and ependymal cells are types of glial cells and the tumor arised from these cells are named according to their origin [7].

1.2.1. Astrocytomas

Astrocytoma, the most common type of brain tumor, arises from astrocytes that are star-shaped cells supportive cells of the brain. It is graded I to IV based on its morphological characteristics. Low grade astrocytomas are localized and grow slowly, while high grade gliomas grow rapidly. Pilocytic astrocytoma (WHO grade I) is the most common type of brain tumor in pediatry. They are located at where they originate and are known as the most benign tumor. Fibrillary astrocytoma (WHO grade II) is low grade brain tumor and it is mostly fatal in adults, since their infiltrative behavior does not allow a total resection. Anaplastic astrocytoma (WHO grade III) is highly malignant that has elevated anaplasia and mitosis than grade II. They have tendency to progress into grade IV astrocytoma. Glioblastoma (GBM, WHO grade IV) is a highly malignant tumor that spreads rapidly into brain tissue. This tumor type is very aggressive and infiltrates brain extensively. Patients have short survival rate due to poor prognosis [7].

1.2.2. Glioblastoma

GBM is the highest grade glioma (WHO grade IV) that is the most malignant type of glioma. It involves 50 per cent of all gliomas and affect mostly adults at ages 45–65. This cancer is observed in men more than women. There are two types of GBM, primary and secondary GBM. Primary GBM derives from normal astrocytes and this type is mostly found in older patients. Secondary GBM develops from a lower grade glioma within five to 10 years of diagnosis [8]. Although they have different progress, they are indistinguishable in morphology and clinical findings. Their histological characteristics of necrosis and elevated blood vessels are used to distinguish GBM from any other grade

glioma. Their progression period from the low grade glioma varies between one year to 10 years [9]. The mean survival outcome of three months has improved to eight months by total resection and the combination of resection and radiation has improved to ten months. Surgery and radiation with temozolomide increase the survival period to 14.6 months [10].

1.3. CELLULAR ENERGY METABOLISM IN GLIOBLASTOMA

1.3.1. Glycolysis

Glucose is taken into cell via membrane embedded proteins, glucose transporters (GLUTs), and degraded into two pyruvate molecules in ten step of glycolysis [11]. Glycolysis starts with the phosphorylation of glucose to glucose-6-phosphate (G6P) by hexokinase 2 (HK2). Glucose-6-phosphate is catalyzed to fructose-6-phosphate (F6P) by phoshoglucose isomerase. F6P is catalyzed to fructose-1,6-biphosphate by phosphofructokinase 1 (PFK1). Then F6P is broken down to dihydroxyacetone phosphate and glyceraldehyde-3-phosphate. Pyruvate and ATP are yielded by pyruvate kinase (PK) with the catalyzation of phosphoenolpyruvate (PEP) in the final step of the glycolysis. In normal cells, pyruvate dehydrogenase (PDH) converts most of the pyruvate to acetyl-CoA, which enters into mitochondria or is transaminated to alanine (Figure 1.1). Two ATP molecules and six NADH molecules are yielded per glucose during a single glycolysis [12]. In contrast to normal astrocytes, GBM cells have differences in their glucose metabolism. Three-fold increase in glycolysis is seen in GBM when their metabolism is compared to normal astrocytes [13].

1.3.1.1. Glucose Transporters

GLUT is activated via oncogenes cMyc, KRas, and HIF-1α and inhibited via tumor suppressor p53 [14]. GLUT3 is activated by IKK/NF-κB axis and inhibited by p53 [15]. Glucose, must be transported through the cell membrane via carrier proteins due to its hydrophilicity. There are fourteen different GLUT proteins in human that are found in different tissues. Regulation of transporters facilitates the rapid proliferation via changing the hexose affinities [16]. Elevated levels of glucose transporters are observed in many

cancer cells as compared to normal tissues. GLUT1, GLUT3, and GLUT12 are found to be overexpressed in brain tumors [17-20]. Glucose transporters are mostly overexpressed at the intermediate zone of the GBM where the tumor cells have higher amounts of HIF-1α and increased hypoxia [21].

1.3.1.2. Hexokinase

Hexokinase (HK) is the first rate-limiting enzyme that has role in glycolysis. Glucose, transported through the cell membrane via corresponding GLUT, is phosphorylated by HK, which is bound to mitochondrial outer membrane via voltage dependent anion channel (VDAC) [22]. HK irreversibly catalyze the phosphorylation of glucose to G6P thus it prevents efflux of glucose. HK has four different isoforms among different mammalian tissues [23]. Their activities can be inhibited by their catalytic product, G6P. Increased glucose uptake in cancer cells is related not only with the upregulation of glucose transporters but also with HKI and HKII isoforms. HKI expressed in normal brain cells and low-grade gliomas [24]. HKII has a higher affinity for glucose and this isoform is often observed as upregulated in GBMs [24,25]. Increased HKII expression is related with poor survival in GBM and radiation-temozolomide treatment [24].

The activity of HK is regulated via p53 based suppression [26]. Aldolase is responsible for the conversion of fructose-1, 6-bisphosphate to glyceraldehyde 3-phosphate and dihydroxyacetone phosphate. P53 and NO enhance gene expression of glycrealdehyde-3-phosphate dehydrogenase (GAPDH) [27]. Acetylation at lysine 254 (K254) increased the activity of GAPDH in relation to glucose amount that is essential for cell proliferation of the tumor cells [28]. Acetylation on GAPDH is reversibly regulated by acetyltransferase PCAF and the deacetylase HDAC5. GAPDH also regulates autophagy of damaged mitochondria [29]. PGAM1 (phosphoglycerate mutase 1) is observed to be increased in gene expression and enzymatic activity in a subset of cancers [30]. Acetylation of PGAM1 elevates its activity, while the activity the deacetylation of *C*-terminal lysine by SIRT1 suppresses its activity [31]. SIRT2 has diverse effects on PGAM1; while SIRT2-based deacetylation decreases PGAM1 activity and inhibits cell proliferation in colon cancer cells (HCT116), it inhibits cell proliferation in lung carcinoma cells (A549) by elevating PGAM1 activity [32,33].

1.3.1.3. Phosphofructokinase

Phosphofructokinase (PFK1) is another rate-limiting enzyme that is allosterically regulated and highly upregulated in tumor cells [34]. In normal cells, PFK1 is inhibited by ATP, but this inhibition is reversed by fructose-2,6-biphosphate (FBP) providing high glycolytic flux [35]. PFK1 expression is observed to be increased in glioma cells, thus has different response to allosteric regulation when glioma cells are compared with normal astrocytes [36]. These differences provide less sensitivity to inhibitory factors and the tumor cells are able to increase their glycolytic rate [37]. On the other hand, PFK2 expression is upregulated in cancer cells to produce more FBP which is the main allosteric regulator of PFK1 that prevents negative allosteric inhibition of ATP on PFK1 [11].

1.3.1.4. Pyruvate Kinase

Pyruvate Kinase (PK) is the last step of the glycolysis that catalyzes the conversion of PEP to pyruvate and produces ATP [38]. Isoform selection and allosteric regulation are responsible for pyruvate synthesis by pyruvate kinase activity. There are four isoforms described for humans; PKL, PKR, PKM1 and PKM2. PKL is located in kidney and liver, while PKR is found in erythrocytes. Adult M1 form (PKM1) is related with normal cells and this isoform is replaced with M2 form (PKM2), which is observed in highly proliferative tumor cells [39,40]. PKM2 oscillates between inactive dimeric and active tetramic forms. This oscillation is regulated with fructose-1,6-biphosphate [41]. The dimeric inactive form of PKM2 slows down the pyruvate formation in order to promote glycolytic intermediates into biosynthetic pathway. The active tetramic form of the PKM2 induces lactate formation from pyruvate. PKM2 is demonstrated to be involved in EGFR signaling pathway which upregulates the expression of PKM2 in GBMs [38,42,43].

1.3.1.5. Lactate Dehydrogenase

Glycolytic product of pyruvate is converted to lactate by lactate dehydrogenase (LDH) in the last step of the glycolysis. This conversion is essential for NAD^+ regeneration in the cytosol to provide the continuity of the glycolysis. There are five different LDH subtypes

(1-5) in mammalian cells [44]. Cellular levels of lactate is determined by different expressions of LDH subunit and lactate monocarboxylate transporter (MCT) in addition to oxidative capacity of cell. LDHA gene, which encodes for LDH5 subunit, is demonstrated to be an essential gene for maintainance and proliferation [45,46]. This gene is controlled by HIF-1α and elevated under hypoxia. HIF-1α is also elevated in many cancers, too [47]. The expression of LDHA and HIF-1α are related with the poor prognosis of cancer [48]. LDHA converting pyruvate into lactate with the help of inhibited PDH activity is elevated in cancer cells [49,50]. They determine the fate of pyruvate at the end of the glycolysis and increase the malignant phenotype of the cancer by Warburg effect [45,51].

LDH is responsible for both forward and backward conversion of pyruvate. LDHA isoform (LDH5) is mostly observed in tumor cells and diverts the conversion of lactate from pyruvate. Upregulation LDH is responsible for maintaining the glycolytic flux via NAD^+ conversion from NADH [37,11]. LDH activity is regulated via phosphorylation and acetylation. The oncogenic receptor tyrosine kinase FGFR1, which is found to be expressed in glioma cells, phosphorylates LDHA at tyrosine sites (Y10 andY83) [52,53]. Phosphorylation of Y10 induces LDHA formation, but phosphorylation at Y83 results in NADH substrate binding [53]. Acetylation at lysine-K-5 leads to the degredation of LDHA by chaperone-mediated autophagy [54].

1.3.1.6. Pyruvate Dehydrogenase

Pyruvate dehydrogenase (PDH) is responsible for the conversion pyruvate into acetyl-CoA and feeding the tricarboxylic acid cycle (TCA). It controls the entry of pyruvate into mitochondria and its activity is regulated by the inhibition of pyruvate dehydrogenase kinase (PDK) (Figure 1.1). PDK2 expression is observed to be increased in GBMs as against normal astrocytes that results with the elevated pyruvate and lactate levels [55]. For further process, pyruvate must be imported into mitochondria by the action of PDH, which is regulated by phosphorylation, free acetyl-CoA levels and NAD^+/NADH ratio [56]. In cancer cells, PDH activity is blocked by the pyruvate dehydrogenase kinase 1 (PDK1) of which activity is triggered by the hypoxia.

1.3.1.7. Monocarboxylate Transporter

Glucose is converted to lactate and then exported out of the cell, thus providing an acidic microenvironment around the cancer cell. This acidification causes cancer cells since to invade and suppress immune system T lymphocytes. Lactate transportation through the cell membrane is supplied by monocarboxylate transporter (MCT) [44]. The lactate produced by a cancer cell is transported out of the cell by MCT4 to protect normal cellular pH. In normal cells, extracellular lactate is taken into oxygenated cell and converted to pyruvate by lactate dehydrogenase B (LDHB). On the other hand, hypoxic cancer cells export lactate molecules leading to acidic cell environment that enhances the cell invasion [12]. Acidity in the extracellular matrix promotes cancer cell motility which results in metastasis and also resistance to chemotherapy and/or radiotherapy [57,58].

1.3.1.8. Hypoxia-Induced Factor-1α

Hypoxia-induced factor-1α (HIF-1α) is a protein that is highly transcribed by reason of hypoxic stress in tumor cells. The downstream product of HIF-1α, GLUT1, is expressed more than normal tissue in the GBM. In this way stem cell phenotype is observed at the core zone of the tumor [59]. HIF-1α activates the vascular endothelial growth factor (VEGF) that contributes vascularization and angiogenesis for the tumor [60]. HIF-1a elevates the expression of PDK1 that inhibits the conversion of acetyl-CoA from pyruvate via inhibition of PDH activity [49]. GLUT3 expression is increased in GBM and this expression level is used for GBM classification [61].

In hypoxia, cancer cells activate and stabilize the transcription factors HIF-1α and HIF-2α, which increase glycolysis and angiogenesis. Stability of HIF-1α promotes the expression of glycolytic proteins and inhibits mitochondrial oxidative phosphorylation proteins. Hexokinase 2 (HK2), which is a main regulator of glycolysis in high grade GBM, is expressed excessively [62-64]. HK2 promotes the activity of aldolase, glyceraldehyde-3-phosphate dehydrogenase, lactate dehydrogenase, and plasma membrane lactate transporters (MCT4), which shifts glucose metabolism towards to glycolysis. Hypoxia with increased glycolysis promotes lactate production in cancer cells [65-68].

1.3.2. Pentose Phosphate Pathway

Bioenergetic resources and macromolecule biosynthesis are required to meet the needs of newly proliferating cells [69]. Most of the macromolecules used during proliferation are produced through *de novo* biosynthesis from glucose [70]. The pentose phosphate pathway (PPP) is a branch of glycolysis that is seperated as oxidative and nonoxidative branches. In oxidative branch of PPP, glucose-6-phosphate (G6P) is dehydrogenated by glucose-6-phosphate dehydrogenase (G6PD) to produce ribose-5-phosphate (R5P), which generates NADPH used as a reducing agent for nucleotide and fatty acid biosynthesis [69,71]. In nonoxidative branch of PPP glycolytic intermediates are converted to ribose-5-phosphate. R5P is a precursor of mainly nucleotides. PPP is elevated in cancer cells in order to provide the need of energy for rapid cell proliferation and the PPP is regulated by oncogenes (PI3K, mTORC1 and K-ras) and tumor suppressors (p53) [71-75].

1.3.3. Tricarboxylic Acid Cycle and Oxidative Phosphorylation

Acetyl-CoA derivatives are used as carbon sources for fatty acids. Since acetyl-CoA cannot transpass the inner membrane of mitochondria, they are synthesized in the mitochondrial matrix. Citrate, combination of acetyl-CoA and oxaloacetate, passes through mitochondrial inner membrane and decomposed into its components by ATP citrate lyase (ACL). Acetyl-CoA is converted to malonyl-CoA by acetyl-CoA carboxylase and both acetyl-CoA and malonyl-CoA are used to synthesize and elongate fatty acid chains by fatty acid synthase (FAS). Oxaloacetate is essential for the synthesis of non-essential amino acids. Glutamine is a carbon source that supplies oxaloacetate to maintain citrate production during TCA cycle [12]. Although the fate of pyruvate depends on many factors, oxygen availability is one of the most important parameter.

Mitochondria provide ATP and metabolic intermediates of macromolecule synthesis. Pyruvate is decarboxylated to acetyl-CoA by pyruvate dehydrogenase (PDH) and acetyl-CoA is the starting point of the TCA cycle in mitochondria (Figure 1.1). Under hypoxia, HIF-1α activates PDK1 and blocks the activity of PDH, conversion of pyruvate to acetyl-CoA. Therefore, HIF-1α suppresses the flow of pyruvate through the TCA cycle [49]. TCA is the main part of the energy production in normal cell metabolism where the lipids,

carbohydrates and proteins were all oxidized. Acetyl-CoA is converted to citrate by citrate synthase and then citrate is transformed to isocitrate by aconitase. Isocitrate is first decarboxylated to α-KG by isocitrate dehydrogenase and then α-KG is decarboxylated to succinyl-CoA by α-KG dehydrogenase. Throughout the activity of these enzymes, CO_2 and $NADH_2$ are produced which will be used for ATP production during ox,dative phosphorylation by electron transport chain complexes (ETC). Succinyl-CoA is then converted to succinate by succinyl-CoA synthetase and GTP is yielded which will be converted to ATP via substrate level phosphorylation. Succinate is converted to fumarate by succinate dehydrogenase and $FADH_2$ is yielded which will be used in ETC. Fumarate is converted to malate by fumarate hydratase and malate is then dehydrated to oxaloacetate by malate dehydrogenase with the production of $NADH_2$. Four-carbon compound oxaloacetate then enters into a condensation reaction with two-carbon compound acetyl-CoA to give a six-carbon citrate (tricarboxylic acid) [76].

Overall under normoxia, ten molecules of NADH and two molecules of $FADH_2$ are produced from a glucose molecule. Reoxidation of the reduced electron carriers is essential for the ATP production in the inner membrane of the mitochondria. Electrons coming from NADH are transferred to oxygen via the passage through respiratory complexes. NADH dehydrogenase (Complex I) is reduced with the electrons coming from NADH and they are transferred to cytochrome *bc*1 complex (Complex III) by reduced coenzyme *Q* (ubiquinone). Succinate dehydrogenase (Complex II) is reduced with the electrons coming from $FADH_2$ and they are transferred to cytochrome *bc*1 complex by reduced coenzyme *Q*. Electrons are transported from cytochrome *bc*1 complex to cytochrome *c* oxidase (Complex IV) by reduced cytochrome *c*. Cytochrome *c* oxidase catalyzes the electron transfer from the cytochrome *c* to oxygen to form H_2O [76].

The mitochondrial respiratory chain complexes associate to form supercomplexes in the mitochondrial inner membrane in order to minimize the ROS production and efficiently transfer electrons to Complex IV [77]. The most common supercomplexes are Complex I/III_n, Complex $I/III_n/IV_n$ and Complex III/IV_n. Complex II is mostly found free but small content of it associates with supercomplexes I/III/IV [78]. Complex I is stabilized with the presence of Complex III and Complex IV and this association is termed as respirasome [79]. In astrocytes, Complex I is found in free state that induce the amount of ROS in astrocytes when they are compared with other brain cells [80].

Elevated levels of macromolecule production in cancer cells results in increase mitochondrial oxidative phosphorylation (OXPHOS) which is responsible for ROS production in the cell. ROS production is elevated with the suppression of pyruvate entry into OXPHOS, which is the result of any inhibition in the ETC system such as mutation, oncogene related suppression or HIF-1α. ROS production is also increased with the slow electron flow against to elevated substrate level [12]. Elevated ROS production in a tumor cells lead to the increase tumor malignancy by inducing genetic instability and resistance to chemotherapy [81].

Brain includes two per cent of all body weight and uses 20 per cent of oxygen consumption. This system utilizes 60 per cent of glucose uptake into the body and needs glucose continuously since brain cannot store the glucose [82]. Normal cells catalyze the citrate through the TCA cycle for ATP production but in cancer cells, citrate and acetyl-CoA are used as a metabolic intermediates which are essential for lipid biosynthesis for rapid proliferation. In GBM, ACL, acetyl-CoA carboxylase (ACACA), and fatty acid synthase are found to be upregulated in GBM [83-85]. In addition to elevated glycolysis, aggressive GBM cells use mitochondrial glucose oxidation *in vivo* to feed the anaplerosis, replenishment of pathway intermediates and biosynthesis. Although GBM cells favor the aerobic glycolysis even the presence of oxygen, they also efficiently produce ATP via mitochondrial respiration [86].

Loss-of-function mutations in OXPHOS genes lead to inactivation of tumor suppressor or activation of pro-oncogenes that induce glycolysis and stabilize the HIF-1α activity [87,88]. Although tumorigenesis promotes the glycolysis with suppressed mitochondrial activity, mitochondria is fully activated in most tumors and OXPHOS fulfills the need of ATP even in the presence of hypoxic conditions [89,90]. In this tumor, cytochromes are fully oxidized for ATP production [91]. Mitochondrial respiration is essential for oncogene-mediated metabolic reprogramming, maintaining the peculiarity of cancer stem cell, promoting drug resistancy and production of the energy for excessive protein translation in tumor cells [92-96]. OXPHOS related energy is also used in cell metastasis when the energy sources are limited for cell motility [97]. OXPHOS regulation is the important in tumor metabolism and is obtained via protein folding quality control. This regulation is provided by the action of mitochondria-localized heat shock protein-90 (HSP90) chaperones and proteases [98,99]. In contrast to normal cells, HSP90 is elevated in most tumor cells to maintain the folding and activity of proteins that have roles in

permeability transition, electron transport chain, citric acid cycle, fatty acid oxidation, amino acid synthesis, and cellular redox status [100].

1.3.4. Fatty Acid Metabolism

Lipid synthesis is important during carcinogenesis since lipids are used for membrane synthesis, energy source, and production of signaling molecules [101].

Most of the carbon for the lipid synthesis is supplied from acetyl-CoA which cannot pass through the mitochondrial membrane. Citrate, the combination of oxaloacetate and acetyl-CoA, is transport into cytoplasm and converted back to acetyl-CoA by ATP citrate lyase (ACL). Acetyl-CoA is then transformed to malonyl-CoA by acetyl-CoA carboxylase. Both malonyl-CoA and acetyl-CoA are used to produce fatty acid chains by fatty acid synthase (FAS) (Figure 1.1). Cytosolic and nuclear acetyl-CoA is used for post translational modification, acetylation, of nonhistone and histone targets [12].

1.3.5. Glutamine Pathway

Glutamine is converted to glutamate by glutaminase-1 enzyme, which is associated with mitochondria [12]. Glutamate is converted to α-KG which enters TCA cycle in mitochondria (Figure 1.1). Glutamate is used for nucleotide synthesis by convertion to aspartate. The elevated glutaminolysis results in alanine and ammonium production [12]. Ninety per cent of glucose and 60 per cent of glutamine is converted into lactate or alanine in GBM cells [102].

Glutaminase (GLS) is located in mitochondria and it is responsible for the production of glutamate from glutamine [103]. GLS expression is found to be elevated in rapidly proliferating cells [104]. Glutamine is an alternative nutrient source that feeds the energy metabolism by entering the Krebs cycle during the aerobic glycolysis. Elevated glutamine is a regulatory factor that enhances the macromolecule production for proliferation and angiogenesis [105]. Glutamate is also an excitatory neurotransmitter which is converted to glutamine by astrocytes for preventing excitotoxic damage. This conversion is not provided in GBM upon lack of related glutamate transporters. GBM also exports glutamate into the cell that enables tumor invasion by causing excitotoxic environment leading to

neuronal dysfunction or loss [106-109]. Normal astrocytes uses ketones derived from fatty acids in the liver by converting them into acetyl-CoA, while GBM cells cannot utilize ketones as a nutrient source due to their dependence on glucose [110-113].

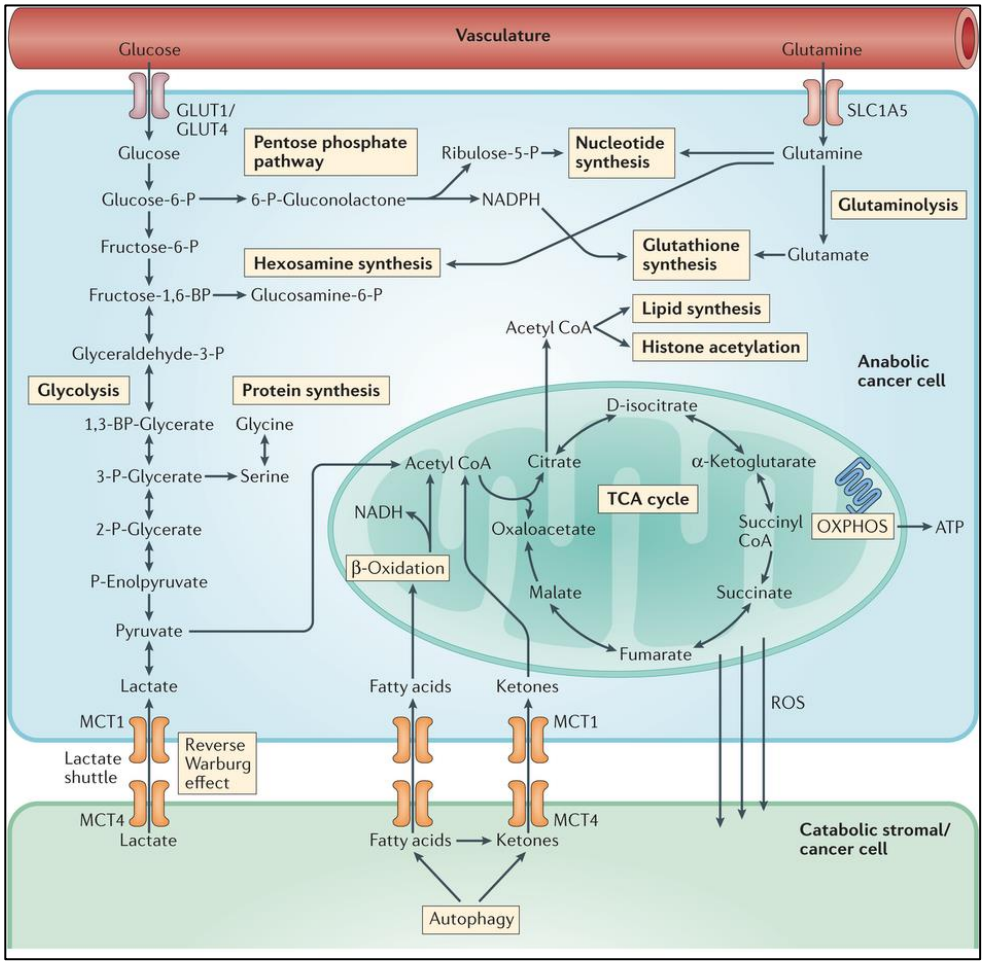

Figure 1.1. Metabolism of a cancer cell [114].

1.4. CANCER RELATED ALTERATIONS IN MITOCHONDRIA

Mitochondria play important roles mainly in cellular metabolism and apoptosis in the cell. Therefore, mitochondrial abnormalities correlate with the changes in energy metabolism, membrane potential regulation, and apoptotic signaling pathways [115,116]. Heterogeneous morphology of gliomas includes mitochondria swelling, partial or total cristolysis, and mitochondrial remodelling. Malignant gliomas have diverse structural changes in their mitochondria at different places around tumor [117]. Structural changes in

mitochondria of gliomas causes alterations in OXPHOS [118,119]. In astrocytomas, lower content of mtDNA correlates with higher malignancy [120].

The difference between the normal and the cancer cells is the need of extracellular stimulation for enhancing the cellular energy pathways. However, cancer cells often have mutations that allow independence for metabolic phenotype [121]. Cancer cells have tumor specific metabolic alterations which are mediated by mutations, enzyme isoforms, post translational modifications, and hypoxia related up or down regulation [122,66,123,124,49,43].

1.4.1. Peroxisome Proliferator-activated Receptor Gamma Co-activator-1 Alpha

Peroxisome proliferator-activated receptor gamma co-activator-1 alpha (PGC-1α) is a transcription factor that regulates mitochondrial biogenesis in the cell [97]. It is activated by the effect of cold, fasting, and exercise when the cell demands large amount of energy [125-127]. PGC-1α enhances mitochondrial oxidative respiration and fatty acid oxidation, while stimulating autophagy under stress conditions [128-132]. PGC-1α activity is controlled by post-translational modifications, phosphorylation and acetylation. Methylation also decreases the stability of PGC-1α [133-135]. PGC-1α is found to be a promoter of carcinogenesis in colon and liver cancers [136]. As in normal cells, PGC-1α regulates OXPHOS and the level of ROS in cancer cells [137].

1.4.2. Isocitrate Dehydrogenase Mutations

Isocitrate dehyrogenase (IDH) catalyzes the decarboxylation of isocitrate and reduces $NADP^+$ to NAPDH. IDH1 is located in cytosol, while IDH2 and IDH3 are located in mitochondria [138,139]. IDH activity is important for controlling the ROS level and maintaining the reduction-oxidation (REDOX) capacity in the cell [44]. IDH is regulated with post-translational modification, acetylation at a specific lysine (K-413) [140]. Cytosolic form of IDH1 is mutated in most of the high grade gliomas [122]. Heterozygous somatic IDH1 mutations at nucleotides that code for arginine (R132) are found in 80 per cent of secondary GBM [141-143], but rarely seen in primary GBM [141,144]. IDH2 mutations in analogous residue to IDH1 (R132), are seldom found in grade II and grade III

gliomas [143]. Both mutations results in nonfunctional enzymes and inability to produce α-KG from isocitrate [145,142] leading to the accumulation of (R)-2-hydroxyglutarate (2-HG), a small oncometabolite [146]. Since α-KG has a role in HIF-1α degredation, IDH is involved in HIF-1α pathway [147]. IDH mutations induce the flux of glutamine into lipid synthesis and inhibiting the OXPHOS with the accumulation of 2-HG, and therefore by favoring anabolic pathways [148,149].

1.4.3. Warburg Effect

Reprogramming of energy metabolism is one of the hallmarks of the cancer. This alteration is based on eliciting the energy need for rapid cell growth and proliferation [150]. In normal cells, energy is firstly obtained via glycolysis in cytoplasm and followed oxidative phosphorylation in mitochondria under normoxia. In hypoxia, normal cells preferably produce energy via glycolysis rather than oxidative phosphorylation. However, cancer cells provide most of the cellular energy through glycolysis even if there is an abundance in oxygen, which is called “Warburg effect“ [151]. Although ATP yield from glycolysis per a glucose molecule is less, the rate of energy production pathway is higher than the one for oxidative phosphorylation [151-153]. Elevated glycolysis is essential in cancer which provides the glycolytic intermediates consumed during cell growth and proliferation [154]. Metabolic reprogramming is not limited with glycolysis, many alterations are indicated in lipid metabolism, amino acid metabolism, hexosamine biosynthetic pathway, mitochondrial biogenesis, and glucose transportation. All of them are the consequences of the alterations in oncogenes and tumor suppressor genes in addition to metabolic enzyme effectors [155]. Proto-oncogene, c-myc, favors glycolysis by regulation of the glycolytic enzymes [156,157]. Transcriptional factor, HIF-1a, is responsible for the aerobic glycolysis via inducing the expression of glycolytic enzymes and inhibiting the TCA cycle and oxidative phosphorylation [158]. Tumor suppressor gene of p53 regulates glycolysis via inhibition of glucose transporters and regulates the glucose metabolism under normoxic or hypoxic conditions [159].

Cellular energy metabolism is one of the major mechanism that is affected during carcinogenesis process. Cancer cells show diverse metabolic anomalies for supporting rapid proliferation [12]. They adapt themselves to maximize the capacity for synthesis of proteins, amino acids, lipids, and nucleic acids. Otto Warburg, demonstrated that cancer

cells use glycolysis rather than OXPHOS even in the presence of oxygen, thus named Warburg effect, as detailed above. This metabolic switch occurs early in the carcinogenic process, before the cancer cells are affected by hypoxia [154]. Increased glycolytic rate is not always related with reduction in OXPHOS activity and mitochondria capacity [160]. In breast and glioma cancers, 80 per cent ATP production is provided by oxidative phosphorylation and 20 per cent from glycolytic reactions [161-163]. There are several benefits that cancer cells prefer glycolysis over mitochondrial oxidation. One of those, ATP production is faster in glycolysis and increased glycolytic rate leads to elevated glycolytic intermediates to meet the biosynthetic needs of *de novo* amino acids, nucleic acids, lipids and NADPH that enhance cell proliferation in cancer cells [153,164,165].

1.5. ANTIGLYCOLYTIC AGENTS

1.5.1. 3-Bromopyruvate

3-Bromopyruvate (3-BrPA) is an alkylating agent that is a pyruvate analogue (Figure 1.2). This agent blocks the activity of GAPDH which is demonstrated as a supporter of tumorigenesis and chemoresistance, related to malignant phenotype of the cancer [166,167]. 3-BrPA is also used in combination treatments upon its cytotoxic effect providing a strategy to overcome drug resistancy. Alkylation on the active site of GAPDH inhibits its activity, and therefore the depletion of ATP and imbalance in redox contribute the cell death [168]. 3-BrPA-based treatment strategies are improved for the treatment of liver, pancreas, and breast cancer models [169].

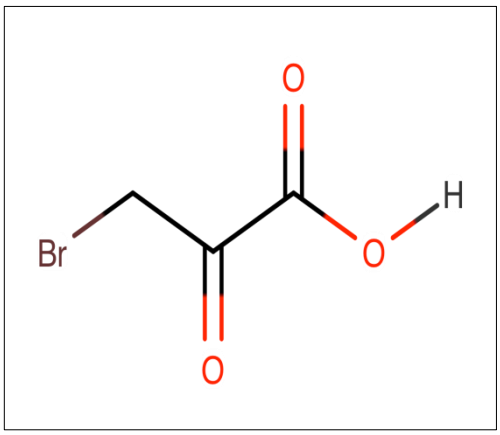

Figure 1.2. The structure of 3-BrPA. It is drawn by MarvinSketch software.

1.5.2. 2-Deoxy-D-Glucose

2-deoxy-D-glucose (2-DG) is a glucose analogue which inhibits the glucose uptake in the cell (Figure 1.3) . When 2-DG is taken into cell, it is phosphorylated by hexokinase into 2-DG-6-phosphate [170,171]. This metabolite cannot be utilized further by enzymes in glycolytic pathway. This results in ATP depletion and induction of apoptosis [172].

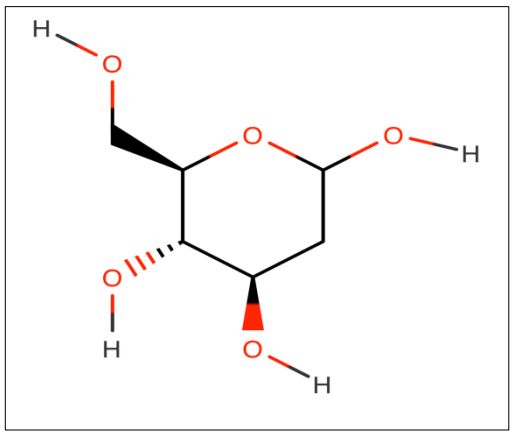

Figure 1.3. The structure of 2-DG. It is drawn by MarvinSketch software.

1.5.3. Dichloroacetate

Dichloroacetate (DCA) is an analogue of acetic acid which has chlorine atoms replaced with two of the hydrogen atoms of methyl group (Figure 1.4). DCA has a form of colorless

crystalline solid with the formula of CH_2Cl_2COOH. DCA salts are used in medicine as a drug for insufficient mitochondria disorder for 25 years [169].

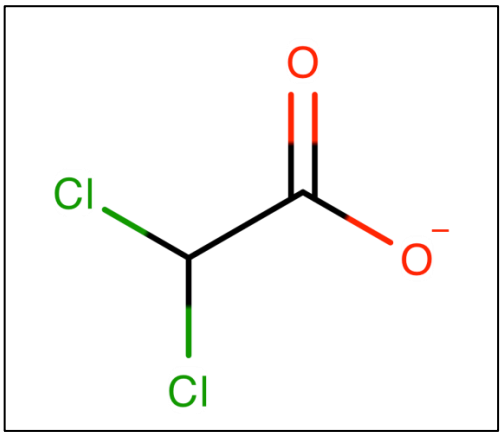

Figure 1.4. The structure of DCA. It is drawn by MarvinSketch software.

Pyruvate dehydrogenase complex (PDC) is responsible for catalysis of the rate-limiting step in aerobic oxidation of glucose, pyruvate, alanine, and lactate to acetyl-CoA [173-176]. PDK isoforms are regulated by reversible phosphorylation that inactivates PDC. DCA mimics the structure of pyruvate and promotes the PDH complex activation by inhibiting the PDK activity. DCA binds hydrophobic part in *N*-terminal domain of PDK and inhibits its interaction with PDK in the presence of ADP [177]. DCA generates conformational changes on PDK1 that inhibits its catalytic activity [178]. DCA also increases the PDC activity upon turnover inhibition. When the drug is orally taken, DCA transports the plasma and mitochondrial membranes by the activity of monocarboxylate and pyruvate transporter system. DCA decreases the lactate production and mitochondrial membrane potential and increases ROS, H_2O_2, and NADH production in mitochondria, which these changes results in decreased cell proliferation and elevated ROS-mediated apoptosis. DCA administration leads to the depolarized mitochondrial membrane potential, activated p53, and suppressed HIF-1α expression [179]. DCA can pass through blood-brain barrier [180,181]. DCA treatment in lung cancer in rats results in the induction of apoptosis and cell proliferation.

Table 1.1. Antiglycolytic agents in cancer from differen studies [168-170]

Compound	Target	Effect	Clinical Status
2-deoxy-D-glucose	Hexokinase, GLUTs	Competitor with glucose	Phase II clinical trials for prostate cancer, Brain toxicity
3-Bromopyruvate	Hexokinase	HK inhibition	Preclinical and clinical trials
Dichloroacetate	Pyruvate Deyhdrogenase Kinase 1	Small molecule inhibitor, PDK inhibition	Phase I clinical trials for brain cancer. PhaseII clinical trials for head-and-neck and non-small cell lung cancers
TLN 232	Pyruvate Kinase 2	Peptidic inhibitor	Precilinical trials and Phase II trials for metastatic Renal Cell Carcinoma and melanoma
Galloflavin	Lactate Dehydrogenase A	LDHA inhibitor	Preclinical trials

1.6. MASS SPECTROMETRY BASED PROTEOMICS

Proteomics is a newly emerging field providing high-throughput profile of proteins at cellular or subcellular levels at a given time and specific conditions. This profiling includes mainly protein expression, post translational modifications, and interactome. Proteins are the functional parts of the cell; therefore, carcinogenesis is influenced by the protein-based changes. Proteomic approaches provide the information about changes in protein localizations, modifications and protein-protein interations in a given biological sample. This technology is used for fingerprinting of protein expression between normal and cancer cells [182] and monitoring cancer-related changes by the identification of diagnostic, prognostic, and predictive biomarkers. Comprehensive protein profiling in glioma is performed by using biospecimens, such as patient biopsies, biological fluids (plasma, serum, and cerebrospinal fluid), glioma cell lines and animal models [183].

Mass spectrometry (MS) is commonly used in protein identification and post-translational modification (PTM) profiling in a biological sample. This technique provides information with higher rate, sensitivity, and accuracy [184-187]. MS-based proteomics provide identification and quantification of proteins in a purified, enriched or complex biological mixture. It is utilized for quantitation of peptide and proteins together with their associated PTMs. MS can also be used to analyze primary structure and proteolytic cleavage sites of the proteins where the *N*- and *C*-terminus of the proteins can be determined. MS is utilized for structural studies of proteins that analyze the conformational data from mass changes [188]. The basic workflow of MS-based approach consists of site-specific enzymatic digestion of proteins, peptide fragmentation through MS, and database analysis via MS/MS fragmented peptide sequence (Figure 1.5) [189].

MS-based approach can identify 10,000 proteins, more than 10,000 phosphorylation sites and more than 3,000 acetylation sites in a single proteome profiling [187].

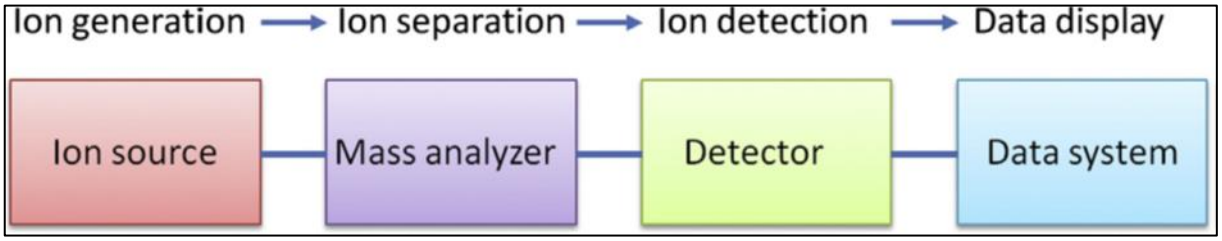

Figure 1.5. The overall flow during mass spectrometry analysis. [187]

1.7. SHOTGUN PROTEOMICS

Shotgun proteomics is a case of bottom-up proteomics which starts with the digestion of proteins into peptides, typically by trypsin (Figure 1.6). Then, complex peptide mixture is analyzed with liquid chromatography which is coupled to tandem mass spectrometry (LC-MS/MS or LC-MALDI MS/MS). Although, shotgun proteomics is a subtype of bottom-up proteomics, it requires LC separation, typically multidimensional LC for digested peptides that is not necessarily for bottom-up proteomics [188]. There are two important factors that limit the protein identification by shotgun MS. The first one is the complexity of cellular proteomes which requires highly sensitive and efficient separation of peptide mixture. The second factor is the dynamic range of proteins which might shadow the overall analysis outcome with demonstration of highly abundant peptides in the peptide/protein mixture.

Proteomic analysis is based on qualitative and/or quantitative analysis and followed by bioinformatic analysis. Qualitative analysis focuses on identifying as many as proteins or PTMs in a given sample.

As a common example for this includes two dimensional liquid chromatography-tandem mass spectrometry (2D-LC-MS/MS). It provides the seperation of tryptic peptides on a cation exchange chromatography (or any corresponding column depending on the sample to be analysed) and detection via mass spectrometry with high sensitivity. Another approach is based on seperation of complex protein sample in the gel,followed by in-gel or in-solution digestion of fractionated proteins and then LC-MS/MS analysis [183].

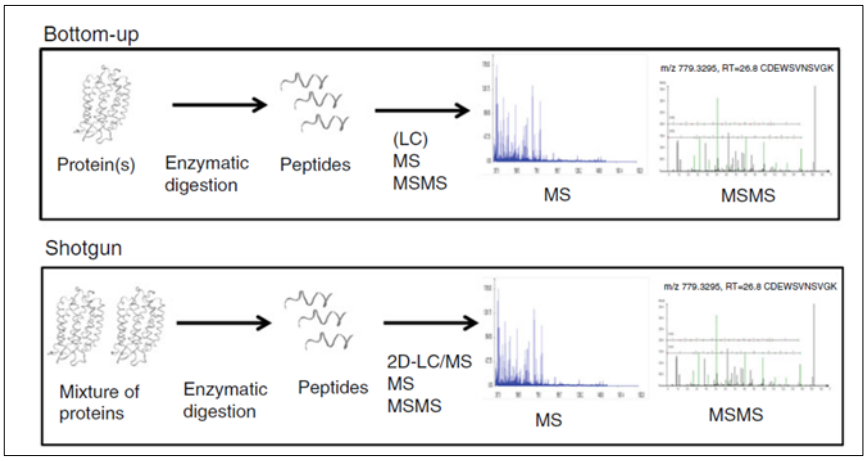

Figure 1.6. Analytic approaches of bottom-up and shotgun proteomics [188].

Quantitative analysis determines the relative or absolute amounts of peptides/proteins in a given sample in order to profile dynamic changes of a specific peptide/protein and PTM. MS-based quantitative strategies can be classified as either stable isotope labeling or label free approaches [190,191]. Stable isotope labeling strategies generate a mass shift by labeling with non-radioactive heavy isotopes that enables the separation identical peptides from different samples within a single MS analysis [185]. Although, they have slightly different molecular weights, chemical properties are mostly identical not changing the ionization efficiency. Mass-to-charge (m/z) difference between two peptides will be observed with mass analysis and the area of each peak will demonstrate the amounts of each peptide[192]. Quantification methods include isotope-coded affinity tags (ICAT), isobaric tags for relative and absolute quantification (iTRAQ), and stable isotope labeling with amino acids in cell culture (SILAC). Label free quantitation compares two or more samples depending on the ion intensities of identical peptides or the number of spectra for

each protein [193]. Samples of label free quantitation are separately prepared and but analyzed on the same LC-MS/MS setup to prevent experiment to experiment variations [193,83]. MS data is analyzed with a bioinformatic tools that submit and analyze the peptide/protein sequences in a database [181]. Mascot and Sequest are the most popular bioinformatic tools for protein identification and PTM mapping. PLGS, X!Tandem, Phenyx, Sonar, and Protein Prospector are also bioinformatic tools that are used for same purpose [194].

MS provides information about the presence of a protein or PTM in a sample [195], but dynamic changes in protein and PTM can also be demonstrated. LC-MS/MS based proteomics is not a quantitative upon difference of tryptic peptides such as peptide length, charge, amino acid content, ion intensities caused by PTM. Thus comparison between different peptides can be applied when peptide mass-to-charge ratios (m/z) are same and obtained under the same conditions during the LC-MS/MS analysis. MS based quantitative strategies can be classified as either stable isotope labeling approaches or label free approaches [195,193]. Stable isotope labeling strategies generate a mass shift by labeling with non-radioactive heavy isotopes that enables the separation identical peptides from different samples within a single MS analysis. Although they have different molecular weights, chemical properties are mostly identical which results with same ionization efficiency. m/z difference between two peptides will be observed with mass analysis and the area of each peak will demonstrate the amounts of each peptide [192]. Relative quantification methods include isotope-coded affinity tags (ICAT), isobaric tags for relative and absolute quantification (iTRAQ), stable isotope labeling with amino acids in cell culture (SILAC). Label free quantitation compares two or more samples depend on the ion intensities of identical peptides or the number of spectra for each protein [193]. Samples of label free quantitation are separately prepared and run but they are run on the same LC-MS/MS setup to prevent setup variations [193].

1.8. AIM OF THE STUDY

Despite many studies about the metabolic differences between normal cells and cancer cells, the carcinogenesis effects on glioblastoma metabolism has not been investigated in detail. In this study, we investigated the metabolic shifts in glioblastoma cellular

metabolism by using U87MG, U373 GBM cancer cell lines and NHA cells for demonstrating the biochemical, mitochondrial, and proteomics alterations between the normal and the glioblastoma cells. We found that GBM cells have increased glycolysis rate with functional OXPHOS capability, which support the malignant phenotype of this brain tumor. These findings about GBM metabolism may be used in further studies as target or combination theraphy with a drug, which can enhance efficiency of the treatment.

2. MATERIALS

2.1. INSTRUMENTS

CO_2 incubator (Nuaire NU5510/E/G, USA), laminar flow cabinet (ESCO Class II Biological Safety Cabinet, AC2-4E8, USA), -80 °C freezer (Thermo Forma -86 C ULT Freezer, USA), light microscope (Nikon Eclipse #TS100, Japan), centrifuge (Beckman Coulter Allegra 25R,USA), centrifuge (Hettich Mikro-22R,Germany), waterbath (Stuart, SB540, UK), vortex (Stuart SA8, UK), pH meter (Hanna instruments PH211, Germany), microplate reader (Bio-Tek EL x 800, USA), Mini-PROTEAN Tetra Cell Electrophoresis System (Bio-Rad #165-8001, USA), Pierce G2 Fast Blotter (Thermo Scientific, #22834, USA), ChemidocTM XRS+ System (Bio-Rad #170-8265, USA), FACSCalibur (Flow Cytometry BD Biosciences #342973), Confocal Microscope (Zeiss LSM 800) are used in this study.

2.2. EQUIPMENTS

Micro pipettes 1000, 200, 100, 10 µl (Eppendorf, Germany), gel loading tips (VWR #37001-152, USA), serological pipettes 25, 10, 5 ml (SPL Life Sciences, Korea), T-25, T-75 cell culture flasks and 6-well, 96-well cell culture plates (Corning, USA), 15ml, 50 ml falcon tubes (Isolab, Germany), cryovials (TPP, Switzerland), hemocytometer (Sigma #Z359629-1EA, Germany), syringe 5 mL (Set Inject, Turkey), 0.22 µm syringe filter (TPP #99722, Switzerland) are used in this study.

2.3. CHEMICALS

Dulbecco’s Modified Eagle’s Medium - High Glucose (Gibco #41966, USA), Dulbecco's Modified Eagle Medium: Nutrient Mixture F-12 (DMEM/F12) (Gibco #10565018, USA), Fetal Bovine Serum (Gibco #10082, USA), Penicillin Streptomycin (Gibco #15070, USA), Amphotericin B (Gibco # 15290018,USA), Trypsin-EDTA 0.25 per cent (Gibco #25200, USA), Dimethyl sulfoxide (DMSO) (SantaCruz #sc-202581, USA), Dulbecco’s Phosphate

Buffered Saline (DPBS) (PAN Biotech #P04-36500, Germany), 2-propanol (AppliChem #A3928, Germany), Methanol 99 per cent (Sigma 34885, USA), Ethanol (AppliChem #A3678, Germany), Ammonium persulfate (APS) (Bio-Rad #162-0700, USA), N,N,N′,N′-23 Tetramethylethylenediamine (TEMED) (SantaCruz #sc-29111, USA), RIPA Lysis Buffer System (SantaCruz #sc-24948, USA), Deacetylation inhibition cocktail (SantaCruz, #sc-362323, USA), Coomassie Blue R250 (Sigma Aldrich # 27816-25G, Germany), Tris Base (MP-Biomedicals #819638, USA), Sodium Dodecyl Sulfate (SDS), (Bio-Rad #161-0302, USA), 30 per cent Acrylamide/Bis Solution, 29:1 (Bio-Rad, #161-0157, USA), Bovine Serum Albumin, (SantaCruz #sc-2323, USA), Glycine (MP-Biomedicals #808822, USA), Glycine (MP-Biomedicals #808822, USA), ProSieveTM QuadColor™ Protein Marker (Lonza, # .00193837, Switzerland), Bromophenol Blue (Sigma Aldrich #114391-5G, Germany), Tween-20 (Merck #8.221.840.500, Germany), β-mercaptoethanol (Merck #8.057.400.250, Germany), Glycerol 99 per cent (HPLC grade) (Sigma #G2025, Germany), Sodium Dichloroacetate (Sigma Aldrich, # 347795, Germany), Mitotracker Green FM (Life Technologies # M7514, USA), Rhodamine 123 (Sigma R8004) are used in this study.

2.4. KITS

BCA Protein Assay Kit (Pierce #23225, USA), DCFDA - Cellular Reactive Oxygen Species Detection Assay Kit (Abcam ab113851, USA), CellTiter 96® AQueous One Solution Cell Proliferation Assay (MTS) (Promega #G358, USA), Clarity Western ECL Substrate (Bio-Rad #170-5061, USA), ATP synthase Specific Activity Microplate Assay Kit (Abcam, ab109716, USA) are used in this experiment.

2.5. ANTIBODIES

LDHA Mouse mAb (Sigma Aldrich # SAB1406077-50UG, Germany), PDK3 Rabbit mAb (Sigma Prestige Antibodies # HPA046583, Germany), β-actin Mouse mAb (SantaCruz #sc-47778, USA), HSP60 Mouse mAb (SantaCruz #sc-271215, USA), Mitoprofile total OXPHOS rodent WB Ab cocktail (Mitosciences #MS604, USA), PGC-1α Rabbit mAb (SantaCruz #sc-13067,USA), Anti-Mouse IgG – Peroxidase Ab (Sigma #A9044,

Germany), and Anti-Rabbit IgG – Peroxidase Ab (Sigma #A6154, Germany) are used in this study.

2.6. CELL LINES

NHA (Normal human astrocytes) and U87MG glioblastoma cell lines were kindly provided by Assist. Prof. Çığır Biray Avcı (Department of Medical Biology, EGE University, Turkey), U373 glioblastoma cell line was provided by Prof. Dr. Mustafa Çulha (Nanotechnology Laboratory, Yeditepe University, Turkey).

.

3. METHODS

3.1. CELL CULTURE

U87MG and U373 glioblastoma cell lines were grown and maintained in Dulbecco's Modified Essential Medium (DMEM) containing 4.5 g/L glucose supplemented with 10 per cent Fetal Bovine Serum (FBS) and one per cent Penicillin-Streptomycin-Amphotericin (PSA) (complete high glucose medium) at 37^0C and five per cent CO_2 in a humidified incubator. NHA was grown and maintained in Dulbecco's Modified Essential Medium : Nutrient Mixture F-12 (DMEM/F12) containing 4.5 g/L glucose supplemented with fifty per cent Fetal Bovine Serum (FBS) and one per cent Penicillin-Streptomycin-Amphotericin (PSA) (complete high glucose medium) at 37^0C and five per cent CO_2 in a humidified incubator.

3.1.1. Thawing Cells From Storage

Cryopreserved cells were taken from -80^oC freezer and immediately warmed until they melt. Cell suspensions were transferred into sterile 15 ml falcon tubes and 5 ml complete high glucose media was added dropwise onto cells to aviod killing the cells. The cell suspensions were cetrifuged at 300 g for 5 minutes to remove the DMSO containing freezing media. Cell pellets were resuspended in complete high glucose media and transferred into a sterile T-25 cell culture flask containing 5 ml of high glucose media. The media of the cells were changed after the cell attached onto flask to remove the rest of the DMSO content. Cells were passaged at least twice before starting the following experiment.

3.1.2. Cell Subculturing

NHA, U87MG and U373 cells were passaged when the cells reached to exactly 80 per cent confluency. Culture medium was removed from the flask and the cells were washed with Phosphate Buffer Saline (PBS, pH 7.4). The cells were treated with 0.25 per cent trypsin-

EDTA (v/v) and incubated at 37^{o}C in an incubator for five minutes. Then the cells were collected in complete high glucose medium to inactivate the trypsin and centifuged 300 g for five minutes. Supernatant was discarded and the cell pellet was resuspended with one mL of dPBS and centrifuged at 300 g for five minutes to remove trypsin content. The cells were resuspended in complete high glucose medium and seeded into tissue culture flasks.

3.1.3. Cryopreservation of the Cells

NHA, U87MG and U373 cells were resuspended with trypsin and counted by using hemocytometer. Counted cells were centrifuged at 300 g for five minutes. Density of cell number for each cryovial was indicated as 1 x 10^6 cells/vial. Supernatant was discarded and the pellets were resuspended in freezing mixture containing 20 per cent FBS (v/v) and 10 per cent DMSO (Dimethyl Sulfoxide) (v/v) and transferred into the cryovial. Cryovials were placed into a isopropanol containing box and frozen at -80^{o}C freezer. For long-term storage, the cryovials were transferred into a liquid nitrogen container.

3.1.4. Sodium Dichloroacetate Treatment

Sodium dichloroacetate was prepared in dPBS, filtered with 0.22 μm syringe filter and diluted in complete high glucose medium to a concentration of 50 mM. Then stock solution was diluted to a concentration of 25 mM, 10 mM, five mM and one mM. In order to analyze the effect of DCA, cells were seeded onto 3 x 24-well-plate with a number of 1.0 x 10^5 cells/well in complete high glucose media. After 24 hours, the medium of each well was changed with DCA containing medium with different concentration (0, 1, 5, 10, 25, 50 mM) and incubated for 24-48-72 hours at 37^{o}C and five per cent CO_2 incubator. Changes in the cell number was observed and recorded under light microscope.

Table 3.1. Dilutions for the required concentrations of DCA treatment.

Concentrations	50 mM DCA Stock	Complete High Glucose Medium
0 mM	0 ml	15 ml
1 mM	0.3 ml	14.7 ml
5 mM	1.5 ml	13.5 ml
10 mM	3 ml	12 ml

25 mM	7.5 ml	7.5 ml
50 mM	15 DCA	0 ml

3.2. BIOCHEMICAL ANALYSIS

3.2.1. Cell Viability Assay

Viability in NHA, U87MG and U373 cells treated with different concentrations of DCA was measured by using CellTiter 96® Aqueous One Solution Cell Proliferation Assay (MTS-[3-(4,5-dimethylthiazol-2-yl)-5-(3-carboxymethoxyphenyl)-2-(4-sulfophenyl)-2H-tetrazolium]). This assay is colorimetric method for determining the number of the viable cells by a tetrazolium compound, which is bioreduced by active cells into a colored formazan product by NADPH or NADH produced by dehydrogenase enzymes. Cells were counted and seeded in three different 96-well-plates with number of 1.0×10^3 cells/well in 100 µl for three days (0, 24h and 48h) in complete high glucose medium. After overnight incubation, medium of the each well was changed with treatment medium. MTS was added into into each well as 10 per cent of the total volume and incubated at 37^0C for two hours in dark. After incubation, absorbance of each sample was measured at 490 nm by a Bio-Tek EL x 800 microplate reader.

3.2.2. Reactive Oxygen Species Detection Assay

The levels of ROS in NHA, U87MG and U373 cells which were exposed to 10 mM DCA treatment were measured by using DCFDA (2',7' –dichlorofluorescin diacetate) Cellular Reactive Oxygen Species Detection Assay Kit, which uses a fluorogenic dye that measures hydroxyl, peroxyl and other ROS activity within the cell. U87MG and U373 cells were seeded in T25 flask and 10 mM DCA treatment was applied on the cells. The control and treated cells were harvested and 1.0×10^5 cells were resuspended in dPBS. Tert-butyl hydroperoxide (TBHP) was applied one of the each cell as a positive control. After treatment, all of the cells were treated with DCFDA fluorogenic dye to measure the ROS

content within the cells for 30 minutes in dark. After incubation the ROS level was measured by FACSCalibur flow cytometer.

3.2.3. ATP Synthase Specific Activity Assay

ATP Synthase Specific Activity Assay Kit was applied in order to analyze the ATP synthase activity by immunocapturing these enyzmes into monoclonal antibody bounded microplate and monitoring the conversion of ATP to ADP by ATP synthase. Cells were grown in T75 cell culture flasks. The cells were harvested and cell pellets were obtained. For lyzing the cells, pellets were exposed to freze-thaw for five times and centrifuged at 12,000 g at 4^{o}C for 30 minutes. Then, the protein concentration of each sample was analyzed by BCA protein assay and the protein concentration of each cells was adjusted to 5.0 mg/mL by adding Solution one supplied with kit. Diluted samples were loaded into monoclonal antibody bound 96-well-plate and incubated at 37^{o}C for one hour. After incubation the wells were emptied and washed by 300 µL of Solution one for two times. 40 µl Lipid Mix was added into each well and incubated at room temperature for 45 minutes. After incubation, 200 µl Reagent Mix was added into each well and the 96-well-plate placed into Bio-Tek EL x 800 microplate reader to measure the absorbance at 340 nm at 30^{o}C by using kinetic program for three hours with the reading interval of a minute.

3.2.4. MitoTracker Green Staining

MitoTracker Green staining was performed for measurement of mitochondrial mass content via mildly thiol-reactive chloromethyl moiety, which is used for mitochondria labeling. Lyophilized MitoTracker Green dye was dissolved in 74 µL DMSO to a final concentration of 1 mM. Then one mM dye was diluted in complete high glucose medium to final concentration of 100 nM for confocal microscopy. NHA, U87MG and U373 cells were seeded onto cover slip which was placed into 6-well-plate with the number of 5.0 x 10^4 in complete high glucose medium. After overnight incubation, each well was emptied and washed with dPBS. 100 nM MitoTracker green dye containing media was added into each well for mitochondrial staining and incubated at 37^{o}C for 10 minutes in dark. After incubation, each well was washed with dPBS for five times with five minute washing

interval. Then the cover slips were placed onto cover slide and images of individual cells were collected by using Zeiss LSM 800 confocal microscope.

3.2.5. Rhodamine Staining

Rhodamine 123 staining was performed for measurement of mitochondrial membrane potential via fluorescent probe for a potent substrate for P-glycoprotein, which is used for mitochondria labeling. Rhodamine 123 dye (one mg/ml) was diluted in complete high glucose medium. NHA, U87MG and U373 cells were seeded onto cover slip which was placed into 6-well-plate with the number of 5.0×10^4 in complete high glucose medium. After overnight incubation, each well was emptied and washed with dPBS. Rhodamine 123 dye containing media was added into each well for mitochondrial staining and incubated at 37^oC for 10 minutes in dark. After incubation, each well of was washed with dPBS for five times with five minute washing interval. Then the cover slips were placed onto cover slide and images of individual cells were collected by using Zeiss LSM 800 confocal microscope.

3.3. PROTEMICS STUDIES

3.3.1. Cell Lysis

Cell pellets collected from NHA, U87MG and U373 cells were lysed with RIPA Lysis Buffer with addition of one per cent protease inhibitor cocktail (PI), one per cent of sodium orthovanadate (Na_3VO_4), one per cent of deacetylation inhibition cocktail. The cell pellets were resuspended with lysis buffer (2 times the pellet volume) and gently pipetted for 4-5 times. The cell pellets were incubated on ice for 10 minutes and centrifuged at 12,000 x g for 10 minutes. The supernatant of the sample was taken into a new 1.5 mL eppendorf tube and BCA assay was performed to determine the protein content of the whole cell lysate. After BCA analysis, 1 µl one per cent of phenylmethanesulfonylfluoride (PMSF) was added into each sample and they were stored at -80^oC.

3.3.2. Bicinchioninic Acid Assay

BCA Proteins Assay was used to measure the protein content in the whole cell lysates. Two mg/ml BSA solution was used as a standard and serial dilution was applied to obtain working range of BSA (0 - 0.125 - 0.25 - 0.5 - 1 - 1.5 - 2 mg/ml). Working Reagent (WR) was prepared according the number of well (200 µL/well) by mixing 50 parts of BCA Reagent A with 1 part of BCA Reagent B (50:1, Reagent A:B). 10 µL of samples and standards were put into 96-well-plate triplicate. 200 µl of WR was put into each well and incubated at 37^{o}C for 30 minutes in dark. After incubation, the absorbance was mesured at 562 nm via Bio-Tek EL x 800 microplate reader. The standard curve was prepared by using absorbance values of BSA standards and the protein content of the samples were calculated according to standard curve.

3.3.3. Immunoblotting

Protein samples of NHA, U87MG and U373 were prepared 25 µg according to BCA assay results and loaded on a 12 per cent SDS-polyacrylamide gel. Proteins were seperated in the gel via SDS-PAGE and they were transferred onto PVDF membrane by using Thermo Scientific Pierce G2 Fast Blotter. Then blocking was applied by using five per cent of skim milk powder in Tris Buffered Saline Tween-20 solution (TBST; 0.1 M Tris-HCl, nine per cent NaCl, 0.1 per cent Tween- 20, pH = 7.4) for 30 minutes. After incubation, the membrane was washed three times with TBST and incubated overnight at 4^{o}C with primary antibody in TBST (MitoProfile Total OXPHOS Rodent WB Antibody Cocktail (1:5000), Lactate Dehydrogenase A antibody (1:500), Pyruvate Dehydrogenase Kinase 3 antibody (1:500), PGC-1α (1:2500), Acetylated Lysine (1:1000). After incubation, the membrane was washed with TSBT for three times and incubated with secondary antibody (anti-mouse or anti-rabbit) for 60 minutes at room temperature on a shaker. After secondary antibody incubation, the membrane was washed for twice with TBST and once with TBS, and then signals are produced with Clarity Western ECL Substrate by imaging with ChemidocTM XRS+ system. The membrane was incubated with β-actin, and HSP60 mouse antibodies prepared in TBST buffer (1:5000) overnight at 4^{o}C as a loading control. After overnight incubation, the membrane was washed with TBST for three times and

incubated with anti-mouse IgG antibody (1:5000) for 60 minutes at room temperature on a shaker. Then, the membrane was washed for two times with TBST and and once with TBS, and monitorized with Clarity Western ECL Substrate by imaging with ChemidocTM XRS+ system. Relative quantitation analysis of the images were performed via ImageLab 5.2.1 software and the values were normalized according to loading control values.

3.3.4. Sample Preparation for Mass Spectrometry-Based Proteomic Analysis

Proteins of NHA and U87MG were separated on a 12 per cent SDS-polyacrylamide gel and stained with coomassie brilliant R250. The protein bands which were selected due to alterations in acetylation immunoblotting were cut out and processed first in washing solution (50 per cent methanol and 5 per cent acetic acid) and then in destaining solution (50 mM amonium bicarbonate and 50 per cent acetonitrile) to take coomassie stain out of gelpieces. Gel pieces were dried in 200 µl acetonitrile. 10 mM dithiotreitol and 100 mM iodoacetamide were added in order to complete protein reduction and alkylation step. For protein digestion, 20 ng/µl tyrpsin solution was added into gel containing tubes and incubated for 16 hours at 37^{o}C. The next day, peptides were extracted and concentrated by using vacuum centrifugation.

3.3.5. Mass Spectrometry Based Analysis

Samples were introduced into Thermo Dionex UltiMate™ 3000 RSLCnano using pre-concentration setup with Acclaim PepMap RSLC C18, 2 µm, 100Å column (Mobile phase A: 100% H2O + 0.1% formic acid, Mobile phase B: 100% acetonitrile + 0.1% formic acid). This separation was followed by Bruker Compact CaptiveSpray NanoBooster-Electrospray-UHR-Quadrupole-Time-of-Flight analyses. Software utilized during the analysis: HyStar3.2 program for the control of whole process, otofControl for MS, Compass Data Analysis for the generation of mgf files and Mascot 2.4.1 based SwissProt database search, Biotools 3.2 to finalize the protein identification process.

3.4. STATISTICAL ANALYSIS

The data were statistically analyzed by using t-test of Microsoft EXCEL 2010 software demonstrated that the data were significant. Each experiment was performed triplicate and p value ≤ 0.05 was considered statistically significant.

4. RESULTS

4.1. BIOCHEMICAL ANALYSIS

4.1.1. Pyruvate Level Measurements of NHA and U87MG Cells

Pyruvate levels of NHA and U87MG whole cell lysates were measured in order to compare the pyruvate content between NHA and U87MG GBM cell line. Therefore, Pyruvate Assay was performed, which oxidizes the pyruvate in the whole cell lysate by pyruvate oxidase and generates color, detected at 570 nm. The pyruvate levels of cells showed a six-times elevation in comparison to control group (Figure 4.1). The experiments were performed triplicate and the results with a value of $p \leq 0.05$ considered significant.

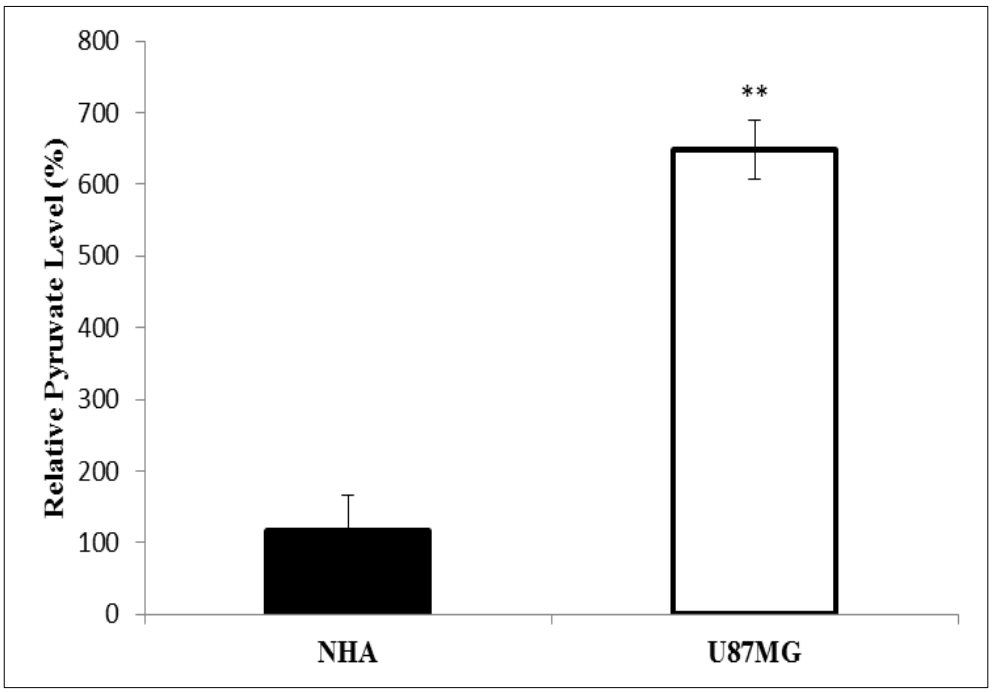

Figure 4.1. Pyruvate level profile comparison between NHA and U87MG glioblastoma cell lines. NHA, and U87MG were seeded into T25 cell culture flask and harvested as a cell pellet. Cell pellets were lysed with extraction buffer and pyruvate measurement was performed according to the manufacturer's instruction. (** denotes for $p \leq 0.01$).

4.1.2. Changes in Lactate Dehydrogenase A Level Between NHA, U87MG and U373 Cells

The changes in the amounts of LDHA were investigated by immunoblotting experiments, samples obtained from NHA, U87MG and U373 cells in order to compare the LDHA content in their whole cell lysate. The signals coming from the LDHA and HSP60 were analyzed by Image Lab.5.1.1 software and the LDHA data were normalized with the data from β-actin signals. According to results, we revealed induction of 250 per cent in both glioblastoma cell lines.

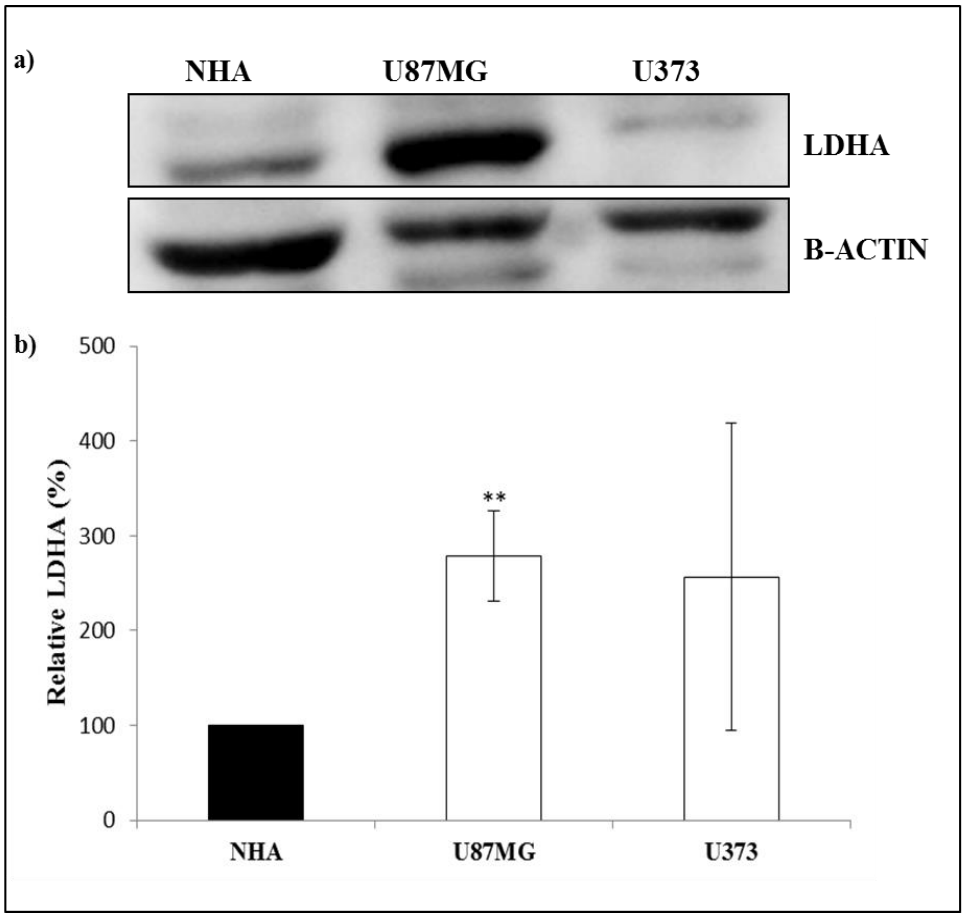

Figure 4.2. Relative changes in LDHA levels of cellular proteins from NHA, U87MG and U373 glioblastoma cell lines. LDHA: Lactate Dehydrogenase A, B-ACTIN: β-actin antibody (** denotes for $p \leq 0.01$). a) Immunoblotting analysis of LDHA and β-actin antibodies, b) Relative changes in LDHA levels.

4.1.3. Changes in Pyruvate Dehydrogenase Kinase 3 Level Between NHA, U87MG and U373 Cells

Immunoblotting analyses of PDK3 were performed in order to reveal the changes in the inhibiton of pyruvate dehydrogenase (PDH), which is responsible for converting cytosolic pyruvate to mitochondrial acetyl-CoA, between NHA and glioblastoma cell lines. The signals coming from the PDK3 and β-actin were analyzed by Image Lab. 5.1.1 software and the PDK3 data were normalized with the data from β-actin signals. According to these findings, we revealed significant elevations in both GBM cells U87MG cells.

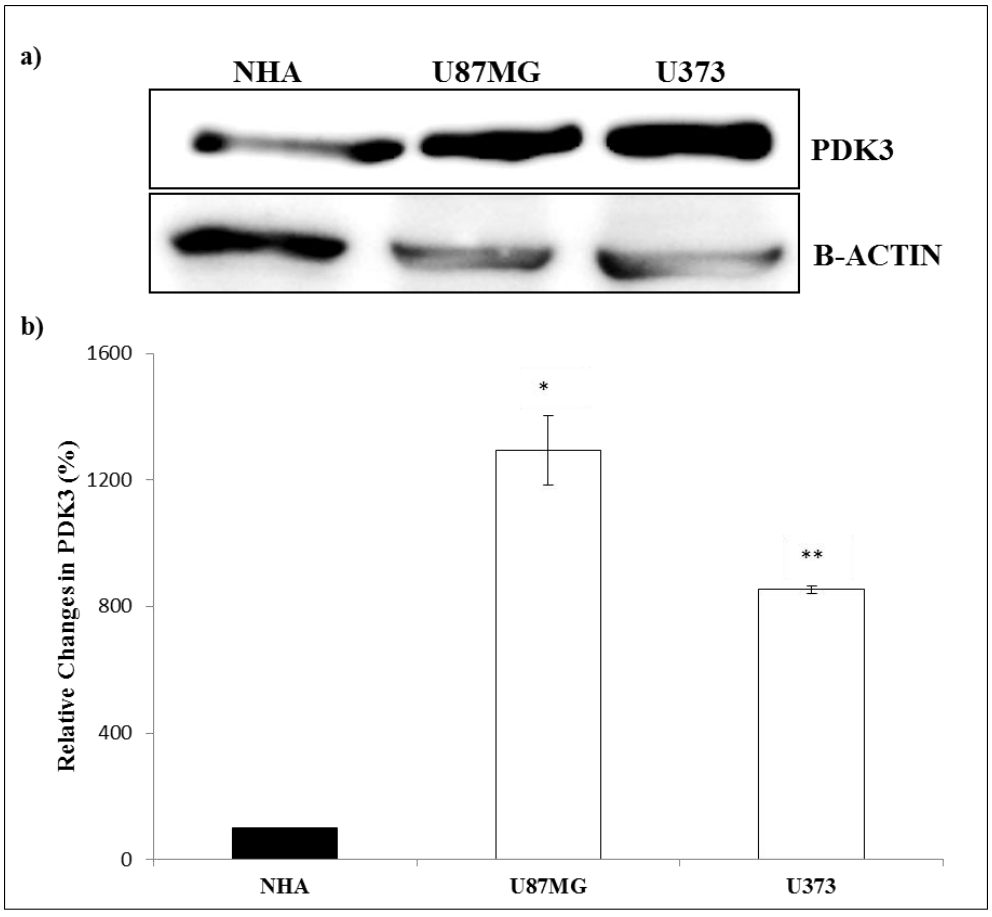

Figure 4.3. Relative changes in PDK3 levels of cellular proteins from NHA, U87MG and U373 glioblastoma cell lines. PDK3: Pyruvate dehydrogenase kinase 3, B-ACTIN: β-actin antibody (* denotes for $p \leq 0.05$). a) Immunoblotting analysis of PDK3 and β-actin antibodies, b) Relative changes in PDK3 levels.

4.2. MITOCHONDRIAL ASSAYS

4.2.1. Changes in Peroxisome Proliferator-Activated Receptor-Gamma Coactivator Among NHA, U87MG and U373 Cells

Immunoblotting analyses of PGC-1α were performed to detect the variations of mitochondrial bioenergetics between NHA and glioblastoma cell lines. The signals coming from the PGC-1α and β-actin were analyzed by Image Lab. 5.1.1 software and the PGC-1α data were normalized with the data from β-actin signals. According to these findings, we revealed increase of 160 per cent in U87MG cells and 172 per cent in U373 cells.

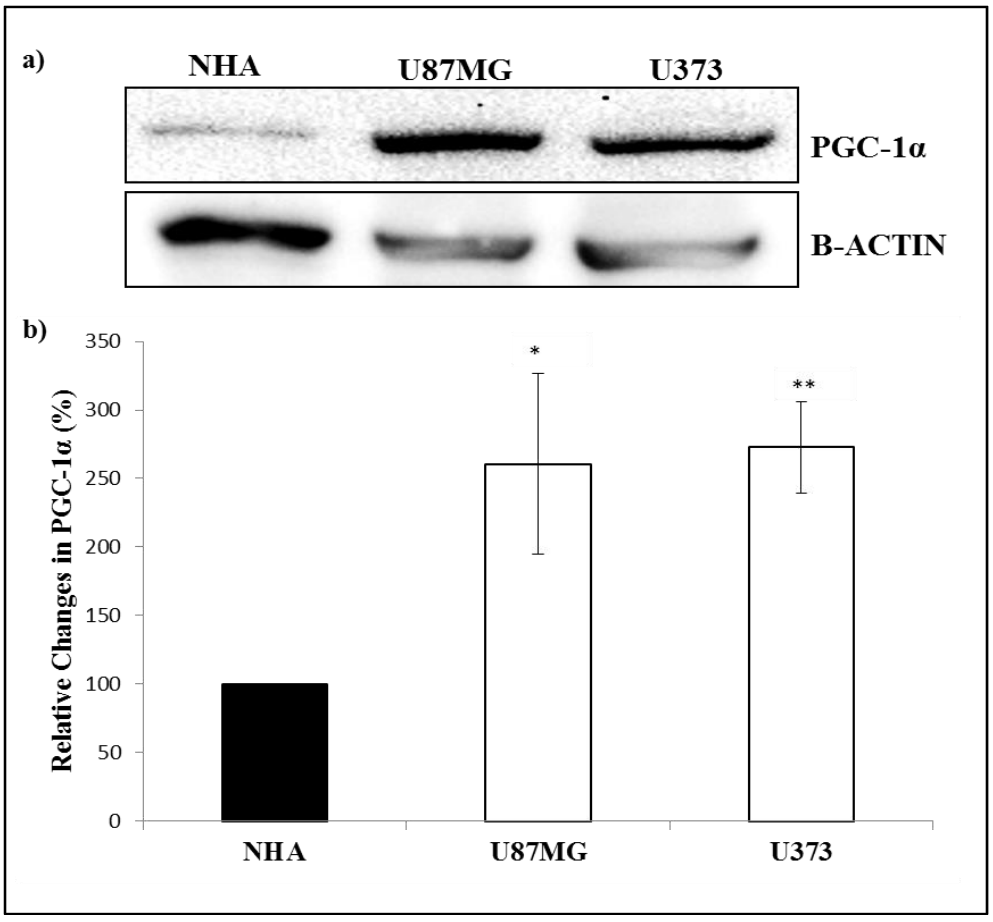

Figure 4.4. Relative changes in PGC-1α levels of cellular proteins from NHA, U87MG and U373 glioblastoma cell lines. PGC-1α: Peroxisome proliferator-activated receptor-gamma coactivator, B-ACTIN: β-actin antibody (* denotes for $p \leq 0.05$, ** denotes for $p \leq 0.01$). a) Immunoblotting analysis of PGC-1α and β-actin antibodies, b) Relative changes in PGC-1α.

4.2.2. Mitochondrial Content Measurements of NHA, U87MG and U373 Cells

MitoTracker Green dye was applied on both normal astrocytes and the glioblastoma cell lines in order to compare the mitochondrial mass content. According to results, both glioblastoma cell lines had elevations in their MitoTracker green fluorescence intensity which is related with mitochondrial mass content. U87MG had 19 per cent increase and U373 had 99 per cent increase when their mitochondrial mass contents were compared with NHA mitochondrial mass content.

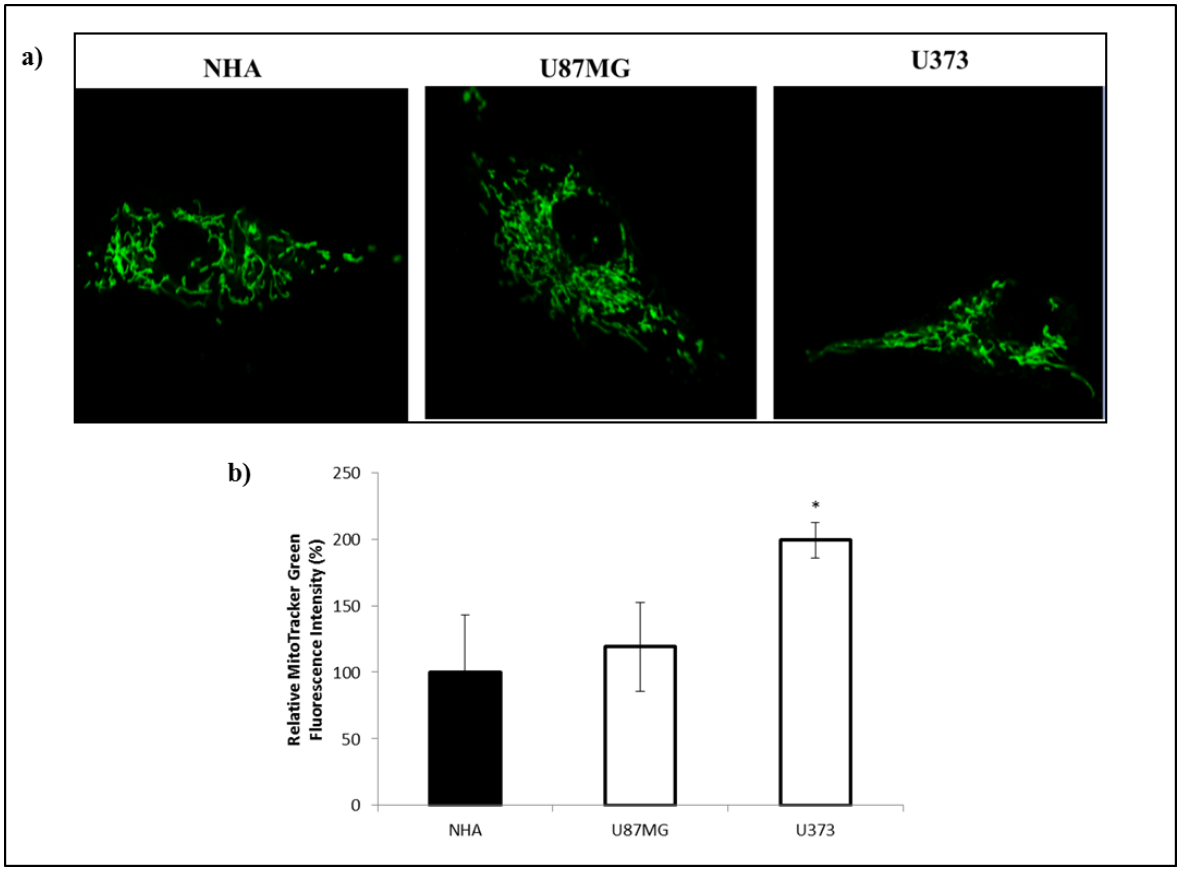

Figure 4.5. Relative variations in mitochondrial mass of NHA, U87MG and U373 cells. Cell were seed on coverslips with the density of 5.0 x 10^5 cells per well inside a 6-well plate. Mitochondria were labeled with a 100-nM MitoTracker Green fluorescent dye in DMEM at 37 °C for 15 min. Stained cells were examined by Zeiss Confocal Microscope with 63X objective lens. a) MitocTracker Green stained cells, b) Relative MitoTracker Green intensity changes.

4.2.3. Mitochondrial Membrane Potential Measurements of NHA, U87MG and U373 Cells

Rhodamine 123 was used to measure mitochondrial membrane potential of NHA, U87MG and U373 cell lines. According to results, we revealed 86 per cent increase in U87MG and 136 per cent increase in U373 mitochondrial membrane potential.

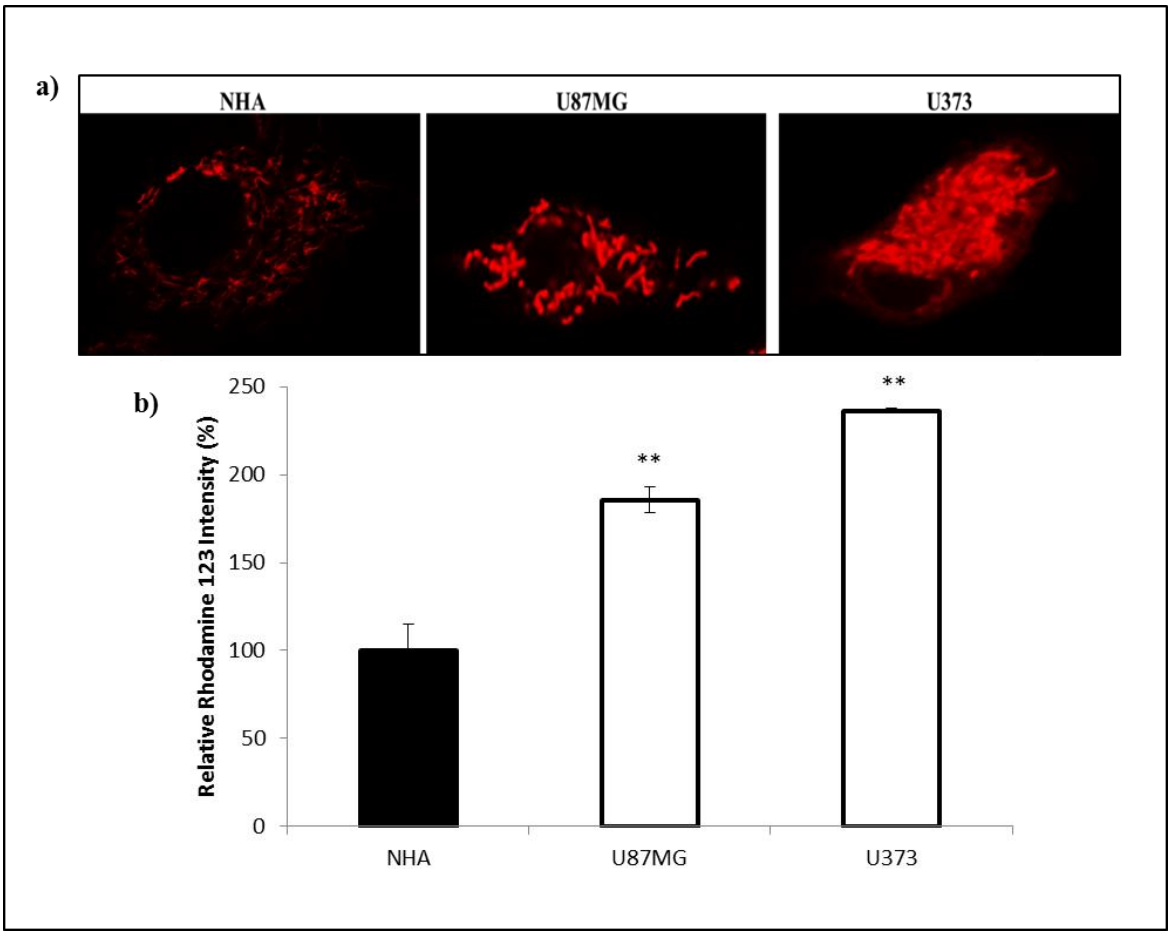

Figure 4.6. Relative changes in mitochondrial membrane potentials of NHA, U87MG and U373 cells. Cells were seed on coverslips with the density of 5.0 x 10^5 cells per well inside a 6-well plate. Mitochondria were labeled with a 1 mg/ml Rhodamine 123 fluorescent dye in DMEM at 37°C for 15 minutes. Stained cells were examined by Zeiss Confocal Microscope with 63X objective lens. a) Rhodamine 123 stained cells, b) Relative Rhodamine 123 intensity changes.

4.2.4. Variations in Electron Transport Chain Complexes of NHA, U87MG and U373 Cells

Changes in the amounts of mitochondrial ETC complexes were investigated by immunoblotting experiments via OXPHOS Rodent WB Antibody Cocktail, by using samples obtained from NHA, U87MG and U373 cells in order to examine the effects of elevated mitochondrial content on ETC complexes. The signals coming from the OXPHOS complexes and HSP60 were analyzed by Image Lab. 5.1.1 software and the OXPHOS complexes data were normalized with the data from HSP60 signals. According to results, we revealed induction of 55 per cent in U87MG cells and 30 per cent in U373 cells in the amount of succinate dehydrogenase (Complex II), 170 per cent increase the amount of Cytochrome bc1 complex (Complex III) in both glioblastoma cell lines, elevation of 100 per cent in U87MG and 120 per cent in U373 cells in the amount of ATP synthase (Complex V).

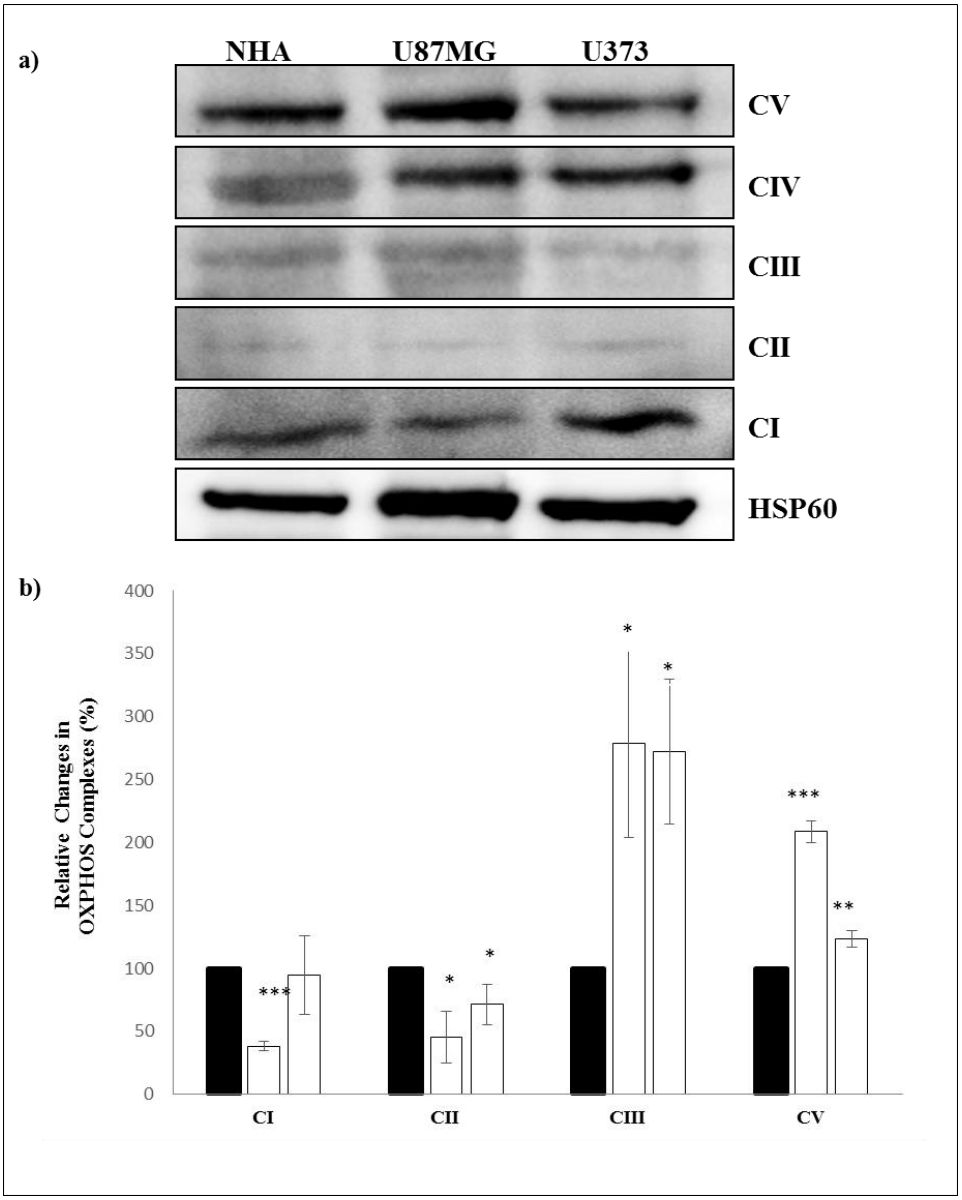

Figure 4.7. Relative alterations of OXPHOS complexes amounts from NHA, U87MG and U373 cells. HSP60: Heat shock protein 60 (kDa); CV: ATP synthase, CIV: Cytochrome c oxidase, CIII; Cytochrome bc1 complex, CII: Succinate dehydrogenase, CI: NADH dehydrogenase (* denotes for $p \leq 0.05$, ** denotes for $p \leq 0.01$, *** denotes for $p \leq 0.001$). a) Immunoblotting analysis of OXPHOS Rodent WB antibody and HSP60 antibodies, b) Relative changes in OXPHOS complexes.

4.2.5. ATP Synthase Specific Activity Measurements of NHA, U87MG and U373 cells

ATP synthase specific activity measurement was performed to whole cell lysate samples of NHA, U87MG and U373 cells in order to examine whether the elevated amount of ATP synthase (Complex V) were functionally active. For this purpose, ATP synthase was immunocaptured within the monoclonal antibody bounded microplate. Then the substrate of this enzyme was added into well and the activity of ATP synthase was detected by measuring optical density, which decreased with the elevation of NAD^+. According to results, we revealed 42 per cent elevation in U87MG and 16 per cent elevation in U373 cells in comparison to NHA cells ATP synthase activity.

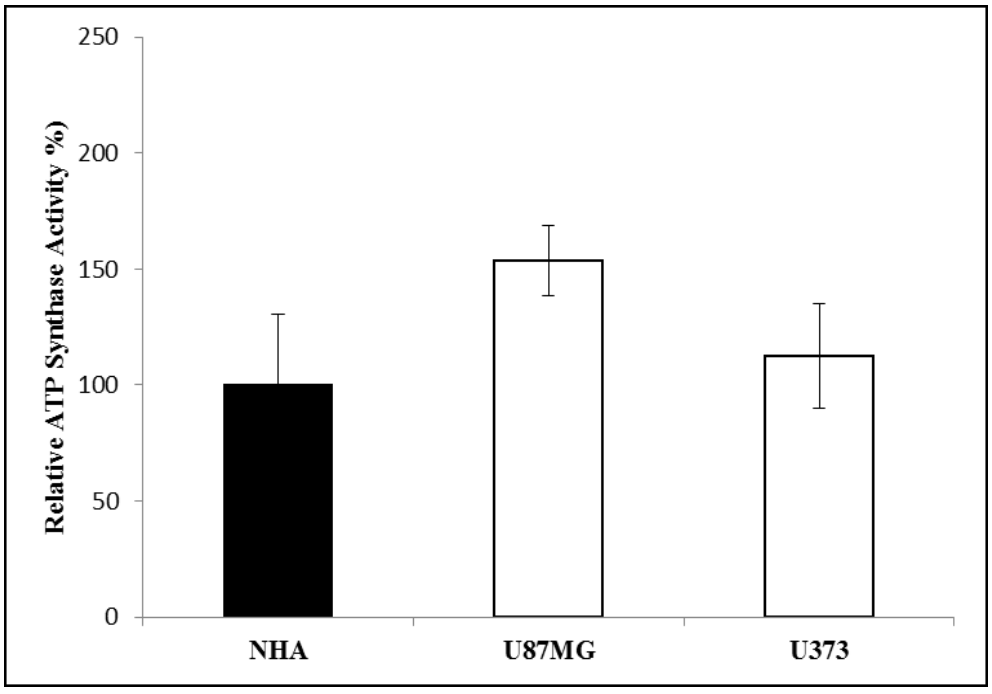

Figure 4.8. ATP synthase activity measurement of NHA, U87MG and U373 cells. ATP synthase from total cell lysates was measured by a kinetic colorimetric assay using the ATP synthase Specific Activity Microplate Assay kit according to the manufacturer's instructions. NHA, U87MG and U373 cells were seeded on T75 cell culture flask and cell pellets were lysed, and the ATP synthase was immune-captured within the 96-well plates.

4.2.6. Cellular Reactive Oxygen Species Measurements of NHA, U87MG and U373 cells

The alterations of ROS level between NHA, U87MG and U373 cells were measured by a DCFDA Cellular ROS Detection Assay Kit, which promotes tumor development and progression. Therefore, a fluorogenic dye 2',7' –dichlorofluorescin diacetate (DCFDA) was used to detect the ROS content, which was taken into cell and oxidized by ROS into 2', 7'– dichlorofluorescein (DCF). DCF was a fluorescent compound and it was detected with maximum excitation and emission spectra of 495 nm and 529 nm. According to results; approximately 2,5 fold increase were revelaed in GBM cells when they were compared with NHA.

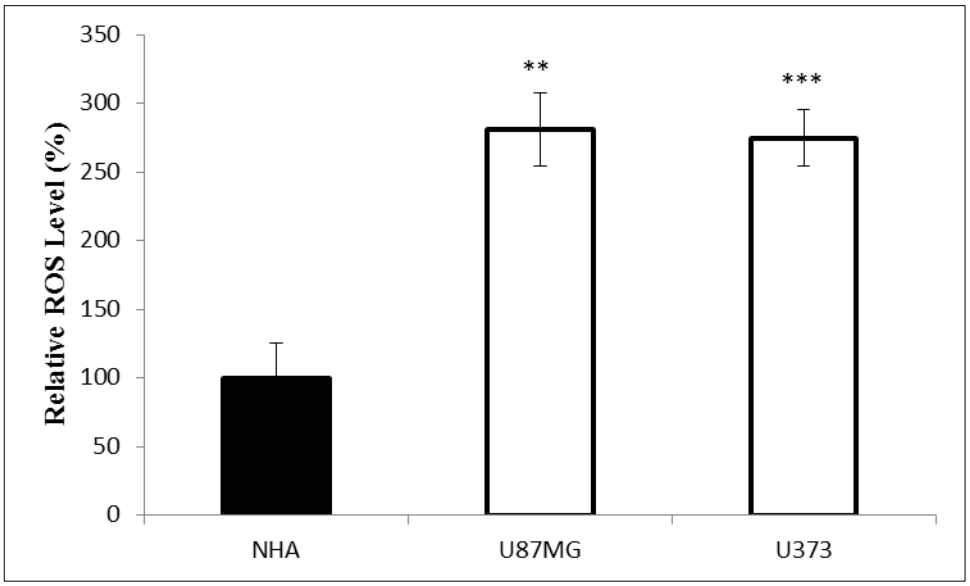

Figure 4.9. Relative alterations in the ROS levels of NHA, U87MG and U373 cells. (** denotes for $p \leq 0.01$, *** denotes for $p \leq 0.001$). NHA, U87MG and U373 cells were incubated with DCFDA and measurement was performed according to the manufacturer's instruction.

4.2.7. DCA Treatment Optimization

The effects of DCA treatment on cell proliferation of NHA, U87MG and U373 cells were measured by MTS cell proliferation assay by exposing different concentration of DCA.

The MTS Tetrazolium compound was oxidized by active cells into colored formazan, which was detected the absorbance at 490nm. We revealed that 10 mM DCA was the lowest concentration which affected both normal and cancer cells significantly. Also, the effect of DCA treatment on cell morphology of NHA, U87MG and U373 cells were observed by using brightfield microscopy.

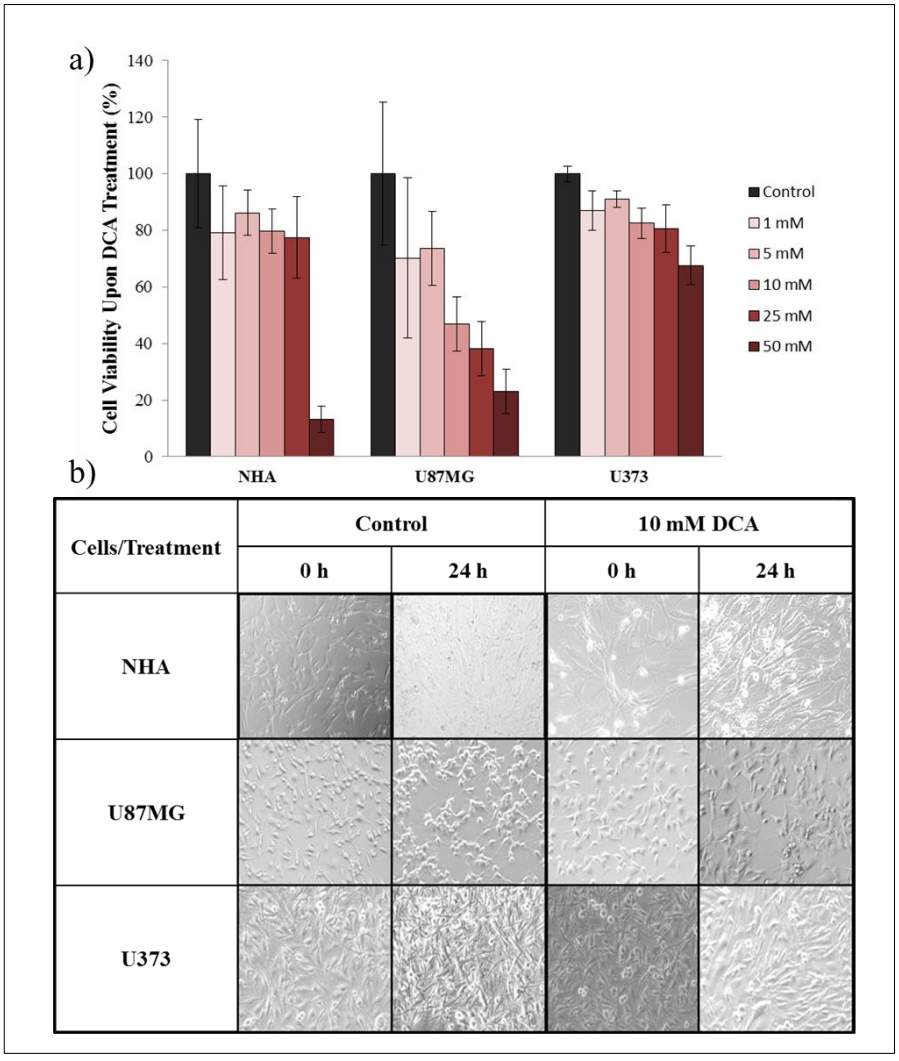

Figure 4.10. The effects of DCA treatment on NHA, U87MG and U373 cells. a) Cell viability results of DCA treatment on NHA, U87MG and U373 cells with different concentrations and interval, b) Cellular morphology of NHA, U87MG and U373 cells upon 10 mM 24 hours treatment.

4.2.8. Effects of DCA Treatment on Electron Transport Chain Complexes

Changes in the amounts of mitochondrial ETC complexes upon 10 mM DCA treatment were investigated by immunoblotting experiments via OXPHOS Rodent WB Antibody Cocktail with samples obtained from NHA, U87MG and U373 cells. The signals coming from the OXPHOS complexes and HSP60 were analyzed by Image Lab. 5.1.1 software and the OXPHOS complexes data were normalized with the data from HSP60 signals. According to results, although we revealed elevation of 20 per cent in U87MG cells and there were not significant alterations in NHA and U373 cells of ATP synthase (Complex V). There was not a change in the amount of Cytochrome bc1 complex (Complex III) in normal human astrocyte but, there both glioblastoma cell lines had decrease upon 10 mM DCA treatment.

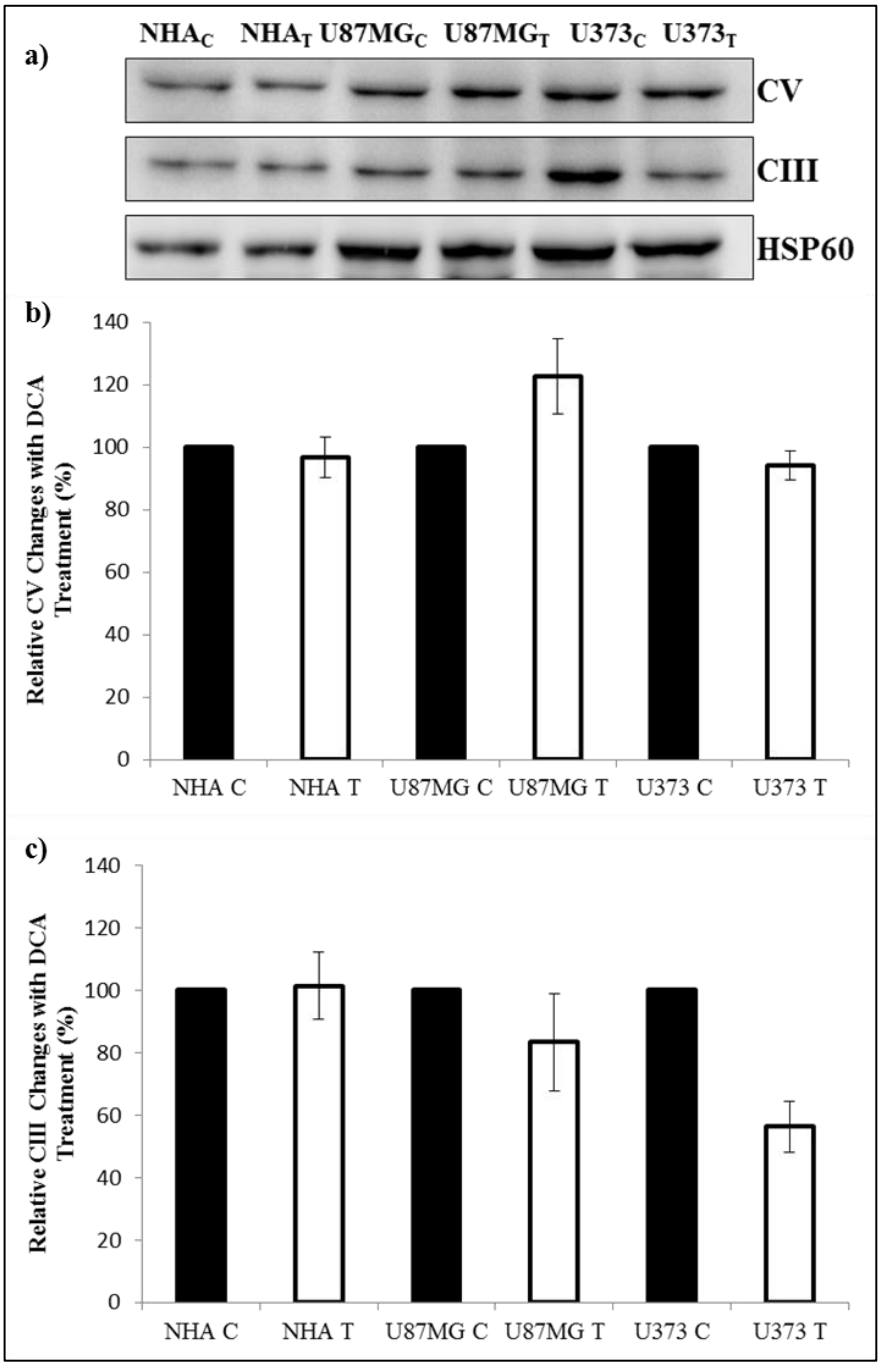

Figure 4.11. Relative changes of OXPHOS complexes amounts of NHA, U87MG and U373 cells upon 10 mM DCA treatment. HSP60: Heat shock protein 60 (kDa); CV: ATP synthase, CIII; Cytochrome bc1 complex. a) Immunoblotting analysis of OXPHOS Rodent WB antibody and HSP60 antibodies, b) Relative changes in Complex V upon DCA treatment, c) Relative changes in Complex III upon DCA treatment.

4.2.9. Changes in ROS Level Upon DCA Treatment

In order to examine the effects of DCA treatment on ROS content, the alterations of ROS level between control and 10 mM DCA treated NHA, U87MG and U373 cells were measured by a DCFDA Cellular ROS Detection Assay Kit. Therefore, a fluorogenic dye 2',7' –dichlorofluorescin diacetate (DCFDA) was used to detect the ROS content, which was taken into cell and oxidized by ROS into 2', 7'– dichlorofluorescein (DCF). DCF was a fluorescent compound and it was detected with maximum excitation and emission spectra of 495 nm and 529 nm.According to results; two fold increase in NHA cells and 10 per cent increase in U87MG cells were revelaed upon 10 mM DCA treatment, but no change was observed in U373 cells.

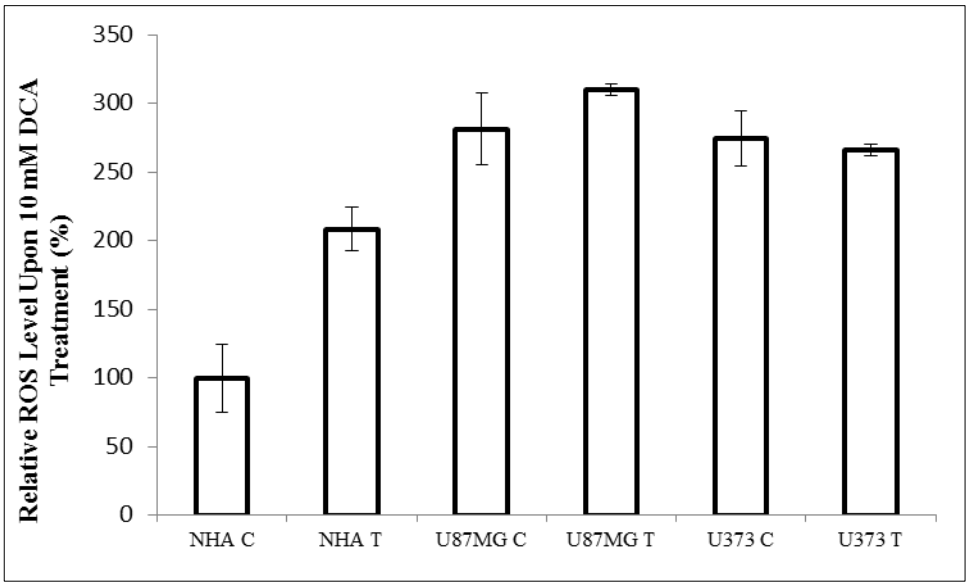

Figure 4.12. The effect of 10 mM DCA treatment on the ROS level of NHA, U87MG and U373 cells. NHA, U87MG and U373 cells were incubated with DCFDA and measurement was performed according to the manufacturer's instruction.

4.3. MASS SPECTROMETRY BASED PROTEOMICS

Changed whole cell proteins of NHA and U87MG were analyzed by MS-based proteomics. Immunoblotting of acetylated proteins of these cells were investigated and two candidate bands were selected for in gel digestion. SDS-PAGE of same samples were

prepared for in gel digestion and one pair of protein band was also added upon the changes in coomasie staining. Three different bands of each sample were in gel digested and analyzed via MS-based approach. According to results, there were metabolic enzymes in the protein candidates.

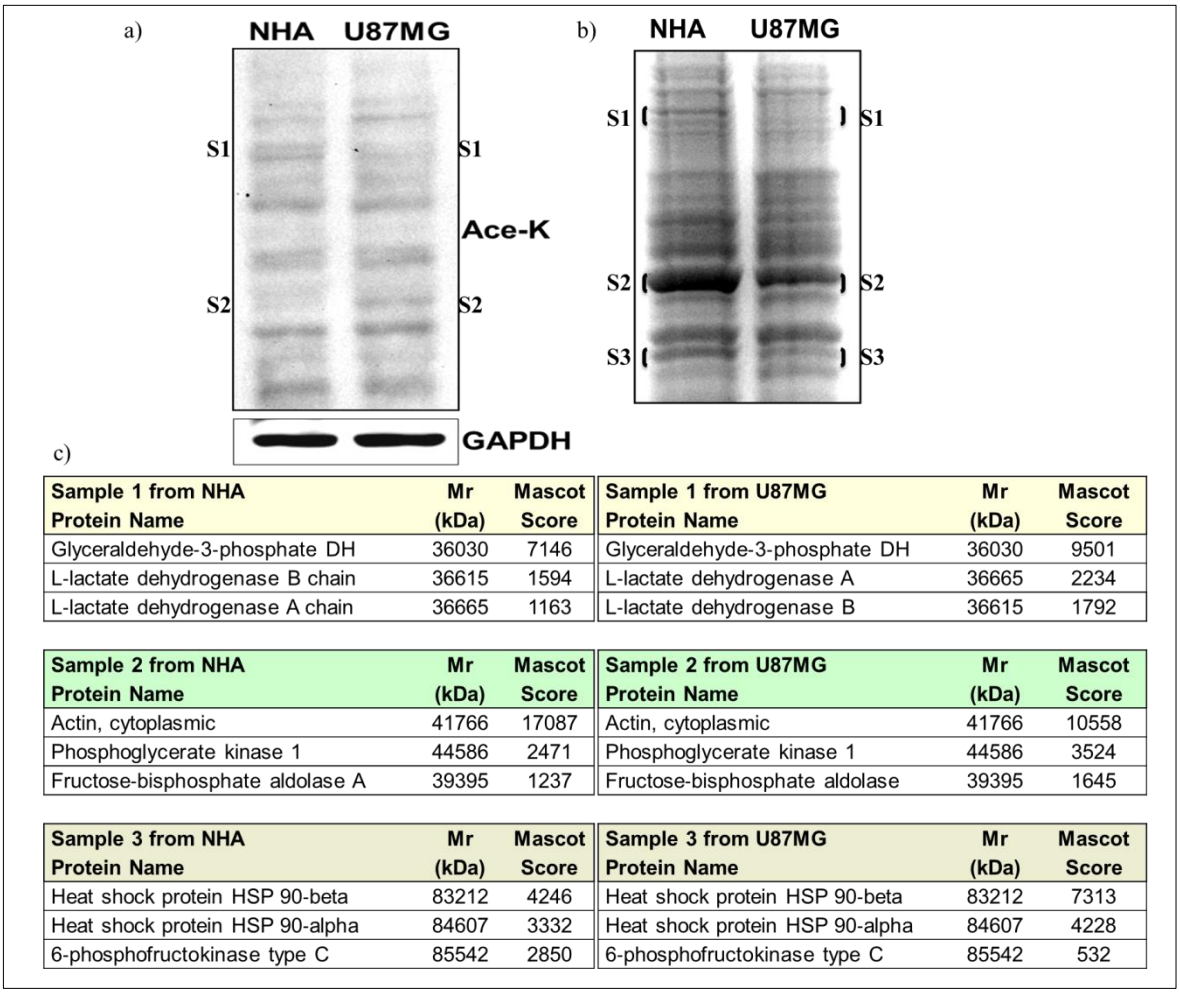

Sample 1 from NHA Protein Name	Mr (kDa)	Mascot Score	Sample 1 from U87MG Protein Name	Mr (kDa)	Mascot Score
Glyceraldehyde-3-phosphate DH	36030	7146	Glyceraldehyde-3-phosphate DH	36030	9501
L-lactate dehydrogenase B chain	36615	1594	L-lactate dehydrogenase A	36665	2234
L-lactate dehydrogenase A chain	36665	1163	L-lactate dehydrogenase B	36615	1792

Sample 2 from NHA Protein Name	Mr (kDa)	Mascot Score	Sample 2 from U87MG Protein Name	Mr (kDa)	Mascot Score
Actin, cytoplasmic	41766	17087	Actin, cytoplasmic	41766	10558
Phosphoglycerate kinase 1	44586	2471	Phosphoglycerate kinase 1	44586	3524
Fructose-bisphosphate aldolase A	39395	1237	Fructose-bisphosphate aldolase	39395	1645

Sample 3 from NHA Protein Name	Mr (kDa)	Mascot Score	Sample 3 from U87MG Protein Name	Mr (kDa)	Mascot Score
Heat shock protein HSP 90-beta	83212	4246	Heat shock protein HSP 90-beta	83212	7313
Heat shock protein HSP 90-alpha	84607	3332	Heat shock protein HSP 90-alpha	84607	4228
6-phosphofructokinase type C	85542	2850	6-phosphofructokinase type C	85542	532

Figure 4.13. MS-based proteomics of NHA and U87MG cells. Software utilized during the analysis: HyStar3.2 program for the control of whole process, otofControl for MS, Compass Data Analysis for the generation of mgf files and Mascot 2.4.1 based SwissProt database search, Biotools 3.2 to finalize the protein ID process. (S1: Sample 1, S2: Sample 2, S3: Sample 3) a) Acetylated proteins of NHA and U87MG cells, b) SDS-polyacrylamide gel and stained with coomassie brilliant R250, c) List of the proteins identified with mass spectrometry-based proteomics

5. DISCUSSION

Glioblastoma is the most malignant brain tumor that has limited lifespan with current treatment [196]. During carcinogenesis, GBM cells undergo a metabolic change for supporting their energy and biomacromolecules needs for rapid cell growth and proliferation [197]. In brain, glial cells are responsible for maintaining the optimal conditions for neuron activity. When they are compared with neurons, the astrocyte cell metabolim favors glycolysis to buffer the pH by taking into the extracellular glutamate to provide neurotransmitter glutamine which show their anerobic glycolysis profile in nature. During carcinogenesis, they change their profile of cell metabolism. In this study, we aimed to reveal the energy metabolism differences between normal human astrocytes and glioblastoma multiforme cells, and also dichloroacetate treatment for manipulating mitochondrial activity.

In order to compare the biochemical profile of NHA and GBM cells, first pyruvate levels were compared by using Pyruvate Assay Kit which showed significant increase in the cellular pyruvate levels in U87MG cells (Figure 4.1). This increase showed that GBM cells have elevated reserves for energy and biomacromolecule productions which can be processed through aerobic glycolysis or oxidative phosphorylation. Increased pyruvate levels also induce angiogenesis in GBM which is driven by HIF-1α via VEGF expression in highly proliferative cancer cells[198].

LDHA is responsible for the conversion of pyruvate to lactate that is the last step of glycolyis. LDHA is upregulated in many cancers which have highly glycolytic phenotype [199]. Therefore, cellular LDHA levels of NHA, U87MG and U373 cells were analyzed via immunoblotting analysis by using LDHA and β-actin antibodies. LDHA levels were elevated in GBM cancer cells when compared with NHA (Figure 4.2). This increase showed that GBM cells have higher capacity for lactate production which supports the aerobic glycolytic phenotype of the GBM cells [199].

Then, PDK3 protein levels of NHA, U87MG and U373 cells were analyzed via immunoblotting of PDK3 and β-actin antibodies which is responsible for pyruvate flow into mitochondria by controlling the activity of PDH. PDK1, is the isoform of PDK3,

levels are elevated in GBM cells when compared with the normal astrocytes [55]. Elevated PDK3 levels in GBM cells were the parts of high glycolytic phenotype of the GBM which could provide carbon fluxes through aerobic glycolysis (Figure 4.3).

Since most of cancer cells have metabolic shift towards the aerobic glycolysis, increase in the glycolytic analyses of GBM cells directed us to consider mitochondrial changes between NHA and GBM cells. First, immunoblotting of PGC-1α was performed to check the levels of mitochondrial biogenesis protein which is upregulated in invasive cancer cells by using PGC-1α and β-actin antibodies [97]. Significant increase in protein levels of PGC-1α in GBM cells was showed that mitochondrial biogenesis was increased (Figure 4.4) during carcinogenesis of astrocytes and it may be the result of the elevated need of metabolic intermediates which are produced during TCA cycle and used in cell proliferation.

Increase in the transcription co-activator, PGC-1α directed us to analyze the mitochondrial content whether this increase affected the mitochondria production in the cancer cells. In order to check the mitochondrial content of NHA and GBM cells, MitoTracker Green staining was performed. According to results, mitochondrial mass content was enhanced in GBM cells when they were compared with NHA (Figure 4.5). Both increases in PGC-1α and MitoTracker Green staining showed that there was an elevation in the mitochondria number of the GBM cells. Anaerobic glycolysis coupled with mitochondrial dysfunction is observed in most of the cancer cells. Then, mitochondrial membrane potential of NHA and GBM cells was analyzed by using Rhodamine 123 dye whether the increase in mitochondrial mass were parallel with functionality. Relative intensity measurements by confocal microscope showed that membrane potential of astrocytes increased during carcinogesis which showed that the increase in the mitochondrial mass did not related to inefficient function of mitochondria in GBM cells (Figure 4.6). In order to analyze the effect of mitochondrial accumulation on ETC complexes in GBM cells, we performed immunoblotting analysis by using MitoProfile Total OXPHOS Rodent WB Antibody Cocktail and HSP60 antibodies. According to results, both GBM cells showed decrease in Complex I and Complex II, also they demonstrated elevation in Complex III and Complex IV when they were compared with NHA (Figure 4.7). Increase in Complex III but decrease in Complex I may be the result of the Complex IV insufficiency that is essential for

supercomplex formation and Complex I stability which is effective for prevention of ROS mediated damage in the cell [80].

Induction in the protein amount in ETC complexes lead us to consider the activity of these complexes of which upregulation may be the result of inefficiency of the complexes. Therefore, ATP synthase activity assay was performed to reveal the activity of Complex V. According to results, a significant increase was found in both GBM cells where the changes was overlapping with the increase in the corresponding proteins (Figure 4.8).

Increased production of ROS is found in many cancers that induces carcinogenesis by promoting genomic instability [200]. To check the effects of carcinogenesis and increased mitochondrial activity on ROS content, DCFDA Cellular Reactive Oxygen Species Detection Assay was performed with NHA and GBM cells. According to results, significant increases were revealed in GBM cells which may be the result of oncogene derived NADPH oxidase-dependent ROS production that is important for cell proliferation (Figure 4.9) [200].

DCA is an antiglycolytic agent that inhibits the activity of PDK which is responsible for the activity of acetyl-CoA converter, PDH. DCA binding results with conformational change and this changes block the activity of PDH which enhance the pyruvate flux into mitochondria. Therefore, DCA was used in order to examine its potential effects on NHA and GBM cells. Different concentrations were applied on NHA and GBM cells in cell viability assay to find the optimized DCA concentration for treatment. According to cell viability assay, 10 mM was selected since it was the lowest and effective concentration that can be used in further assays (Figure 4.10). Next, immunoblotting analysis was performed by using MitoProfile Total OXPHOS Rodent WB Antibody Cocktail and HSP60 antibodies to investigate the effects of 10 mM DCA on ETC complexes. According to results, there were not significant alterations in NHA and U373 cells but increase was found in Complex V of U87MG cells. Also, it was revealed that 10 mM DCA affected only GBM cells in Complex III rather than NHA (Figure 4.11). This data was very interesting since DCA should induce the flux of pyruvate through the mitochondria but it was revealed that there was a limitation in the amount of mitochondrial proteins. This might be the result of the effects of DCA on supercomplexes in mitochondria. In order to check the effects of 10 mM DCA treatment on cellular ROS content, DCFDA Cellular Reactive Oxygen Species Detection Assay was performed. According to results, there was

a significant increase in NHA but there were not significant changes in GBM cells (Figure 4.12). This might be the result of the DCA effects of different ROS sources in the cells which the analysis did not provide only the mitochondria mediated ROS but also other sources [200].

Proteins are functional parts of the cells which are affected during the carcinogenesis. Therefore, we performed a MS-based proteomic approach for identifying candidate proteins which were related with GBM formation. In order to determine the changed proteins between NHA and U87MG, whole cell acetylation was investigated by immunoblotting via acetylation and β-actin antibodies since the metabolic enzyme activities are regulated via PTMs and acetylation is one of them. Changed acetylation bands were selected for in-gel trypsin digestion step. According to MS based proteomic analysis results, there were changes on different metabolic proteins, such as GAPDH, LDHA, LDHB, and HSP90 that participate in glycolysis and OXPHOS which were directly affected during GBM formation (Figure 4.13).

6. CONCLUSION AND FUTURE PERSPECTIVE

Glioblastoma is a highly malignant brain tumor which has cellular adaptations that enable and enhance the survival skills of astrocytes during the cancer formations. In this study, it was shown that GBM cells increased not only their glycolytic capacity but also OXPHOS rate essential for meeting the needs of energy and biomacromolecules for their rapid proliferation and angiogenesis. Pyruvate levels, LDHA and PDK3 protein expression levels, which are implied in glycolytic pahtway, were elevated in both GBM cells. PGC-1α, mitochondrial mass and membrane potential of both GBM cells were elevated during carcinogenesis process, which affected ETC complexes by changing their supercomplex distribution. Also GBM cells demonstrated increase in ATP synthase activity which is responsible for the production of most of the ATP utilized. These metabolic phenotypes showed that both GBM cell line does not display Warburg effect as their metabolic modulations. Dichloroacetic acid (DCA) treatment affected the cell proliferation and the supercomplex distributions in mitochondria of GBM cells, which provided toleration to DCA treatment in cancer cells by supressing DCA mediated ROS generation. In addition, this study demonstrated that cancer formation changes the protein profile of the cells of astrocytes, related to cellular energy metabolism. LDHA, LDHB, GAPDH, PGK1, ALDOA, and PFK-C were identified as the major candidate proteins affected during gliomagenesis though mass spectrometry-based proteomics approach.

These metabolic profiling provided an understanding in a part of the metabolic shift between normal astrocytes and GBM cells. Further studies for comprehensive analysis of metabolic alterations are needed for advancements in the manipulation of cancer metabolism. DCA treatment is an effective approach for rapid GBM proliferation but the mechanism of DCA mediated apoptosis must be studied whose effects on ROS could not be seen by cellular ROS analysis. The candidate proteins which were provided by MS-based proteomics must be confirmed by further immunoblotting assays.

REFERENCES

1. F. Erbsloh, A. Bernsmeier and H. Hillesheim. The Glucose Consumption of the Brain and Its Dependence on the Liver. *Archiv fur Psychiatrie und Nervenkrankheiten, Vereinigt Mit Zeitschrift fur die Gesamte Neurologie und Psychiatrie*, 196:611-626, 1958.

2. P. Mergenthaler, U. Lindauer, G. A. Dienel and A. Meisel. Sugar for the Brain: the Role of Glucose in Physiological and Pathological Brain Function. *Trends in Neurosciences*, 36:587-597, 2013.

3. I. A. Simpson, A. Carruthers and S. J. Vannucci. Supply and Demand in Cerebral Energy Metabolism: the Role of Nutrient Transporters. *Journal of Cerebral Blood Flow and Metabolism : Official Journal of the International Society of Cerebral Blood Flow and Metabolism*, 27:1766-1791, 2007.

4. G. A. Dienel. Fueling and Imaging Brain Activation. *ASN Neuro*, 4, 2012.

5. D. A. Turner and D. C. Adamson. Neuronal-astrocyte Metabolic Interactions: Understanding the Transition into Abnormal Astrocytoma Metabolism. *Journal of Neuropathology and Experimental Neurology*, 70:167-176, 2011.

6. W. H. Organization. GLOBOCAN 2012. http://globocan.iarc.fr/Default.aspx [retrieved 15 October 2016].

7. F. Ali-Osman. *Brain Tumors*. Humana Press Inc, New Jersey, 2005.

8. F. B. Furnari, T. Fenton, R. M. Bachoo, A. Mukasa, J. M. Stommel, A. Stegh, W. C. Hahn, K. L. Ligon, D. N. Louis, C. Brennan, L. Chin, R. A. DePinho and W. K. Cavenee. Malignant Astrocytic Glioma: Genetics, Biology, and Paths to Treatment. *Genes and Development*, 21:2683-2710, 2007.

9. H. Ohgaki, K. Watanabe, A. Peraud, W. Biernat, A. von Deimling, M. G. Yasargil, Y. Yonekawa and P. Kleihues. A Case History of Glioma Progression. *Acta Neuropathologica*, 97:525-532, 1999.

10. R. Altieri, A. Agnoletti, F. Quattrucci, D. Garbossa, F. M. Calamo Specchia, M. Bozzaro, R. Fornaro, C. Mencarani, M. Lanotte, R. Spaziante and A. Ducati. Molecular Biology Of Gliomas: Present and Future Challenges. *Translational Medicine UniSa*, 10:29-37, 2014.

11. L. Yu, X. Chen, L. Wang and S. Chen. The Sweet Trap in Tumors: Aerobic Glycolysis and Potential Targets for Therapy. *Oncotarget*, 2016.

12. S. K. Marie and S. M. Shinjo. Metabolism and Brain Cancer. *Clinics*, 1:33-43, 2011.

13. S. Oudard, F. Arvelo, L. Miccoli, F. Apiou, A. M. Dutrillaux, M. Poisson, B. Dutrillaux and M. F. Poupon. High Glycolysis in Gliomas Despite Low Hexokinase Transcription and Activity Correlated to Chromosome 10 Loss. *British Journal of Cancer*, 74:839-845, 1996.

14. L. K. Boroughs and R. J. DeBerardinis. Metabolic Pathways Promoting Cancer Cell Survival and Growth. *Nature Cell Biology*, 17:351-359, 2015.

15. K. Kawauchi, K. Araki, K. Tobiume and N. Tanaka. p53 Regulates Glucose Metabolism Through an IKK-NF-Kappab Pathway and Inhibits Cell Transformation. *Nature Cell Biology*, 10:611-618, 2008.

16. A. J. Cura and A. Carruthers. The Role of Monosaccharide Transport Proteins in Carbohydrate Assimilation, Distribution, Metabolism and Homeostasis. *Comprehensive Physiology*, 2:863-914, 2012.

17. M. L. Macheda, S. Rogers and J. D. Best. Molecular and Cellular Regulation of Glucose Transporter (GLUT) Proteins in Cancer. *Journal of Cellular Physiology*, 202:654-662, 2005.

18. A. Godoy, V. Ulloa, F. Rodriguez, K. Reinicke, A. J. Yanez, L. Garcia Mde, R. A. Medina, M. Carrasco, S. Barberis, T. Castro, F. Martinez, X. Koch, J. C. Vera, M. T. Poblete, C. D. Figueroa, B. Peruzzo, F. Perez and F. Nualart. Differential Subcellular Distribution of Glucose Transporters GLUT1-6 and GLUT9 in Human Cancer: Ultrastructural Localization of GLUT1 and GLUT5 in Breast Tumor Tissues. *Journal of Cellular Physiology*, 207:614-627, 2006.

19. R. J. Boado, K. L. Black and W. M. Pardridge. Gene Expression of GLUT3 and GLUT1 Glucose Transporters in Human Brain Tumors. *Molecular Brain Research*, 27:51-57, 1994.

20. F. Stockhammer, A. von Deimling, M. Synowitz, C. Blechschmidt and F. K. van Landeghem. Expression of Glucose Transporter 1 is Associated with Loss of Heterozygosity of Chromosome 1p in Oligodendroglial Tumors WHO Grade II. *Journal of Molecular Histology*, 39:553-560, 2008.

21. F. Pistollato, E. Rampazzo, L. Persano, S. Abbadi, C. Frasson, L. Denaro, D. D'Avella, D. M. Panchision, A. D. Puppa, R. Scienza and G. Basso. Interaction of HIF1α and Notch Signaling Regulates Medulloblastoma Precursor Proliferation and Fate. *Stem Cells*, 28:1918-1929, 2010.

22. S. P. Mathupala, Y. H. Ko and P. L. Pedersen. Hexokinase II: Cancer's Double-Edged Sword Acting as Both Facilitator and Gatekeeper of Malignancy When Bound to Mitochondria. *Oncogene*, 25:4777-4786, 2006.

23. J. E. Wilson. Isozymes of Mammalian Hexokinase: Structure, Subcellular Localization and Metabolic Function. *The Journal of Experimental Biology*, 206:2049-2057, 2003.

24. A. Wolf, S. Agnihotri, J. Micallef, J. Mukherjee, N. Sabha, R. Cairns, C. Hawkins and A. Guha. Hexokinase 2 is a Key Mediator of Aerobic Glycolysis and Promotes Tumor Growth in Human Glioblastoma Multiforme. *The Journal of Experimental Medicine*, 208:313-326, 2011.

25. T. A. Smith. Mammalian Hexokinases and Their Abnormal Expression in Cancer. *British Journal of Biomedical Science*, 57:170-178, 2000.

26. H. R. Kim, J. S. Roe, J. E. Lee, E. J. Cho and H. D. Youn. p53 Regulates Glucose Metabolism by miR-34a. *Biochemical and Biophysical Research Communications*, 437:225-231, 2013.

27. J. Y. Zhang, F. Zhang, C. Q. Hong, A. E. Giuliano, X. J. Cui, G. J. Zhou, G. J. Zhang and Y. K. Cui. Critical Protein GAPDH and Its Regulatory Mechanisms in Cancer Cells. *Cancer Biology and Medicine*, 12:10-22, 2015.

28. T. Li, M. Liu, X. Feng, Z. Wang, I. Das, Y. Xu, X. Zhou, Y. Sun, K. L. Guan, Y. Xiong and Q. Y. Lei. Glyceraldehyde-3-phosphate Dehydrogenase is Activated by Lysine 254 Acetylation in Response to Glucose Signal. *The Journal of Biological Chemistry*, 289:3775-3785, 2014.

29. A. Colell, J. E. Ricci, S. Tait, S. Milasta, U. Maurer, L. Bouchier-Hayes, P. Fitzgerald, A. Guio-Carrion, N. J. Waterhouse, C. W. Li, B. Mari, P. Barbry, D. D. Newmeyer, H. M. Beere and D. R. Green. GAPDH and Autophagy Preserve Survival After Apoptotic Cytochrome c Release in the Absence of Caspase Activation. *Cell*, 129:983-997, 2007.

30. X. Jiang, Q. Sun, H. Li, K. Li and X. Ren. The Role of Phosphoglycerate Mutase 1 in Tumor Aerobic Glycolysis and Its Potential Therapeutic Implications. *International Journal of Cancer*, 135:1991-1996, 2014.

31. W. C. Hallows, W. Yu and J. M. Denu. Regulation of Glycolytic Enzyme Phosphoglycerate Mutase-1 by Sirt1 Protein-Mediated Deacetylation. *The Journal of Biological Chemistry*, 287:3850-3858, 2012.

32. T. Tsusaka, T. Guo, T. Yagura, T. Inoue, M. Yokode, N. Inagaki and H. Kondoh. Deacetylation of Phosphoglycerate Mutase in Its Distinct Central Region by SIRT2 Down-Regulates Its Enzymatic Activity. *Genes to Cells : Devoted To Molecular and Cellular Mechanisms*, 19:766-777, 2014.

33. Y. Xu, F. Li, L. Lv, T. Li, X. Zhou, C. X. Deng, K. L. Guan, Q. Y. Lei and Y. Xiong. Oxidative Stress Activates SIRT2 to Deacetylate and Stimulate Phosphoglycerate Mutase. *Cancer Research*, 74:3630-3642, 2014.

34. J. Deprez, D. Vertommen, D. R. Alessi, L. Hue and M. H. Rider. Phosphorylation and Activation of Heart 6-Phosphofructo-2-Kinase by Protein Kinase B and Other Protein Kinases of the Insulin Signaling Cascades. *The Journal of Biological Chemistry*, 272:17269-17275, 1997.

35. B. Clem, S. Telang, A. Clem, A. Yalcin, J. Meier, A. Simmons, M. A. Rasku, S. Arumugam, W. L. Dean, J. Eaton, A. Lane, J. O. Trent and J. Chesney. Small-molecule Inhibition of 6-phosphofructo-2-kinase Activity Suppresses Glycolytic Flux and Tumor Growth. *Molecular Cancer Therapeutics*, 7:110-120, 2008.

36. J. E. Dominguez, J. F. Graham, C. J. Cummins, D. J. Loreck, J. Galarraga, J. Van der Feen, R. DeLaPaz and B. H. Smith. Enzymes of Glucose Metabolism in Cultured Human Gliomas: Neoplasia is Accompanied by Altered Hexokinase, Phosphofructokinase, and Glucose-6-phosphate Dehydrogenase Levels. *Metabolic Brain Disease*, 2:17-30, 1987.

37. D. Stieber, S. A. Abdul Rahim and S. P. Niclou. Novel Ways to Target Brain Tumour Metabolism. *Expert Opinion on Therapeutic Targets*, 15:1227-1239, 2011.

38. S. Mazurek, C. B. Boschek, F. Hugo and E. Eigenbrodt. Pyruvate Kinase Type M2 and Its Role in Tumor Growth and Spreading. *Seminars in Cancer Biology*, 15:300-308, 2005.

39. Z. J. Reitman, G. Jin, E. D. Karoly, I. Spasojevic, J. Yang, K. W. Kinzler, Y. He, D. D. Bigner, B. Vogelstein and H. Yan. Profiling the Effects of Isocitrate Dehydrogenase 1 and 2 Mutations on the Cellular Metabolome. *Proceedings of the National Academy of Sciences of the United States of America*, 108:3270-3275, 2011.

40. S. M. Ronnebaum, O. Ilkayeva, S. C. Burgess, J. W. Joseph, D. Lu, R. D. Stevens, T. C. Becker, A. D. Sherry, C. B. Newgard and M. V. Jensen. A Pyruvate Cycling Pathway Involving Cytosolic NADP-Dependent Isocitrate Dehydrogenase Regulates Glucose-

stimulated Insulin Secretion. *The Journal of Biological Chemistry*, 281:30593-30602, 2006.

41. S. Mazurek, H. Grimm, C. B. Boschek, P. Vaupel and E. Eigenbrodt. Pyruvate Kinase Type M2: a Crossroad in the Tumor Metabolome. *The British Journal of Nutrition*, 87:23-29, 2002.

42. S. Mazurek. Pyruvate Kinase Type M2: a Key Regulator of the Metabolic Budget System in Tumor Cells. *The International Journal of Biochemistry and Cell Biology*, 43:969-980, 2011.

43. H. R. Christofk, M. G. Vander Heiden, M. H. Harris, A. Ramanathan, R. E. Gerszten, R. Wei, M. D. Fleming, S. L. Schreiber and L. C. Cantley. The M2 Splice Isoform of Pyruvate Kinase is Important for Cancer Metabolism and Tumour Growth. *Nature*, 452:230-233, 2008.

44. C. Li, G. Zhang, L. Zhao, Z. Ma and H. Chen. Metabolic Reprogramming in Cancer Cells: Glycolysis, Glutaminolysis, and Bcl-2 Proteins as Novel Therapeutic Targets for Cancer. *World Journal of Surgical Oncology*, 14:15, 2016.

45. V. R. Fantin, J. St-Pierre and P. Leder. Attenuation of LDH-A Expression Uncovers a Link Between Glycolysis, Mitochondrial Physiology, and Tumor Maintenance. *Cancer Cell*, 9:425-434, 2006.

46. H. Shim, C. Dolde, B. C. Lewis, C. S. Wu, G. Dang, R. A. Jungmann, R. Dalla-Favera and C. V. Dang. c-Myc Transactivation of LDH-A: Implications for Tumor Metabolism and Growth. *Proceedings of the National Academy of Sciences of the United States of America*, 94:6658-6663, 1997.

47. I. F. Robey, A. D. Lien, S. J. Welsh, B. K. Baggett and R. J. Gillies. Hypoxia-Inducible Factor-1α and the Glycolytic Phenotype in Tumors. *Neoplasia*, 7:324-330, 2005.

48. Y. Yao, H. Wang and B. Li. LDH5 Overexpression Is Associated With Poor Survival In Patients With Solid Tumors: A Meta-Analysis. *Tumor Biology*, 35:6973-6981, 2014.

49. J. Kim, I. Tchernyshyov, G. L. Semenza and C. V. Dang. HIF-1-mediated Expression of Pyruvate Dehydrogenase Kinase: A Metabolic Switch Required for Cellular Adaptation to Hypoxia. *Cell Metabolism*, 3:177-185, 2006.

50. C. V. Dang and G. L. Semenza. Oncogenic Alterations of Metabolism. *Trends in Biochemical Sciences*, 24:68-72, 1999.

51. A. Le, C. R. Cooper, A. M. Gouw, R. Dinavahi, A. Maitra, L. M. Deck, R. E. Royer, D. L. Vander Jagt, G. L. Semenza and C. V. Dang. Inhibition of Lactate Dehydrogenase A Induces Oxidative Stress and Inhibits Tumor Progression. *Proceedings of the National Academy of Sciences of the United States of America*, 107:2037-2042, 2010.

52. T. Ueba, J. A. Takahashi, M. Fukumoto, M. Ohta, N. Ito, Y. Oda, H. Kikuchi and M. Hatanaka. Expression of Fibroblast Growth Factor Receptor-1 in Human Glioma and Meningioma Tissues. *Neurosurgery*, 34:221-225; 225-226, 1994.

53. J. Fan, T. Hitosugi, T. W. Chung, J. Xie, Q. Ge, T. L. Gu, R. D. Polakiewicz, G. Z. Chen, T. J. Boggon, S. Lonial, F. R. Khuri, S. Kang and J. Chen. Tyrosine Phosphorylation of Lactate Dehydrogenase A Is Important for NADH/NAD+ Redox Homeostasis in Cancer Cells. *Molecular and Cellular Biology*, 31:4938-4950, 2011.

54. D. Zhao, S. W. Zou, Y. Liu, X. Zhou, Y. Mo, P. Wang, Y. H. Xu, B. Dong, Y. Xiong, Q. Y. Lei and K. L. Guan. Lysine-5 Acetylation Negatively Regulates Lactate Dehydrogenase A and Is Decreased in Pancreatic Cancer. *Cancer Cell*, 23:464-476, 2013.

55. E. D. Michelakis, G. Sutendra, P. Dromparis, L. Webster, A. Haromy, E. Niven, C. Maguire, T. L. Gammer, J. R. Mackey, D. Fulton, B. Abdulkarim, M. S. McMurtry and K. C. Petruk. Metabolic Modulation of Glioblastoma With Dichloroacetate. *Science Translational Medicine*, 2:31-34, 2010.

56. R. Curi, P. Newsholme and E. A. Newsholme. Metabolism of Pyruvate by Isolated Rat Mesenteric Lymphocytes, Lymphocyte Mitochondria and Isolated Mouse Macrophages. *The Biochemical Journal*, 250:383-388, 1988.

57. T. Shiraishi, J. E. Verdone, J. Huang, U. D. Kahlert, J. R. Hernandez, G. Torga, J. C. Zarif, T. Epstein, R. Gatenby, A. McCartney, J. H. Elisseeff, S. M. Mooney, S. S. An and K. J. Pienta. Glycolysis Is the Primary Bioenergetic Pathway for Cell Motility and Cytoskeletal Remodeling in Human Prostate and Breast Cancer Cells. *Oncotarget*, 6:130-143, 2015.

58. S. Peppicelli, F. Bianchini and L. Calorini. Extracellular Acidity, A "Reappreciated" Trait of Tumor Environment Driving Malignancy: Perspectives in Diagnosis and Therapy. *Cancer Metastasis Reviews*, 33:823-832, 2014.

59. A. K. Rooj, A. Bronisz and J. Godlewski. The Role of Octamer Binding Transcription Factors in Glioblastoma Multiforme. *Biochimica et Biophysica Acta*, 1859:805-811, 2016.

60. V. A. Carroll and M. Ashcroft. Role of Hypoxia-Inducible Factor (HIF)-1alpha Versus HIF-2alpha In the Regulation of HIF Target Genes In Response to Hypoxia, Insulin-like Growth Factor-I, or Loss of Von Hippel-Lindau Function: Implications for Targeting the HIF Pathway. *Cancer Research*, 66:6264-6270, 2006.

61. W. A. Flavahan, Q. Wu, M. Hitomi, N. Rahim, Y. Kim, A. E. Sloan, R. J. Weil, I. Nakano, J. N. Sarkaria, B. W. Stringer, B. W. Day, M. Li, J. D. Lathia, J. N. Rich and A. B. Hjelmeland. Brain Tumor Initiating Cells Adapt To Restricted Nutrition Through Preferential Glucose Uptake. *Nature Neuroscience*, 16:1373-1382, 2013.

62. I. Marin-Valencia, C. Yang, T. Mashimo, S. Cho, H. Baek, X. L. Yang, K. N. Rajagopalan, M. Maddie, V. Vemireddy, Z. Zhao, L. Cai, L. Good, B. P. Tu, K. J. Hatanpaa, B. E. Mickey, J. M. Mates, J. M. Pascual, E. A. Maher, C. R. Malloy, R. J. Deberardinis and R. M. Bachoo. Analysis of Tumor Metabolism Reveals Mitochondrial Glucose Oxidation in Genetically Diverse Human Glioblastomas in the Mouse Brain *in vivo*. *Cell Metabolism*, 15:827-837, 2012.

63. D. J. Brat and T. B. Mapstone. Malignant Glioma Physiology: Cellular Response to Hypoxia and Its Role in Tumor Progression. *Annals of Internal Medicine*, 138:659-668, 2003.

64. G. L. Wang, B. H. Jiang, E. A. Rue and G. L. Semenza. Hypoxia-inducible Factor 1 Is A Basic-Helix-Loop-Helix-PAS Heterodimer Regulated by Cellular O_2 Tension. *Proceedings of the National Academy of Sciences of the United States of America*, 92:5510-5514, 1995.

65. H. M. Said, C. Hagemann, A. Staab, J. Stojic, S. Kuhnel, G. H. Vince, M. Flentje, K. Roosen and D. Vordermark. Expression Patterns of the Hypoxia-Related Genes Osteopontin, CA9, Erythropoietin, VEGF and HIF-1alpha in Human Glioma *in vitro* and *in vivo*. *Radiotherapy and Oncology : Journal of the European Society for Therapeutic Radiology and Oncology*, 83:398-405, 2007.

66. G. L. Semenza, B. H. Jiang, S. W. Leung, R. Passantino, J. P. Concordet, P. Maire and A. Giallongo. Hypoxia Response Elements in the Aldolase A, Enolase 1, and Lactate Dehydrogenase A Gene Promoters Contain Essential Binding Sites for Hypoxia-Inducible Factor 1. *The Journal of Biological Chemistry*, 271:32529-32537, 1996.

67. M. S. Ullah, A. J. Davies and A. P. Halestrap. The Plasma Membrane Lactate Transporter MCT4, But Not MCT1, Is Up-Regulated by Hypoxia Through A HIF-1alpha-Dependent Mechanism. *The Journal of Biological Chemistry*, 281:9030-9037, 2006.

68. S. E. Rademakers, J. Lok, A. J. van der Kogel, J. Bussink and J. H. Kaanders. Metabolic Markers In Relation To Hypoxia; Staining Patterns and Colocalization of Pimonidazole, HIF-1alpha, CAIX, LDH-5, GLUT-1, MCT1 and MCT4. *BMC Cancer*, 11:167, 2011.

69. R. G. Jones and C. B. Thompson. Tumor Suppressors and Cell Metabolism: A Recipe for Cancer Growth. *Genes and Development*, 23:537-548, 2009.

70. D. E. Bauer, G. Hatzivassiliou, F. Zhao, C. Andreadis and C. B. Thompson. ATP Citrate Lyase Is An Important Component of Cell Growth and Transformation. *Oncogene*, 24:6314-6322, 2005.

71. P. Jiang, W. Du and M. Wu. Regulation of the Pentose Phosphate Pathway in Cancer. *Protein and Cell*, 5:592-602, 2014.

72. V. Nogueira and N. Hay. Molecular Pathways: Reactive Oxygen Species Homeostasis in Cancer Cells and Implications for Cancer Therapy. *Clinical Cancer Research : An Official Journal of the American Association for Cancer Research*, 19:4309-4314, 2013.

73. P. Jiang, W. Du, X. Wang, A. Mancuso, X. Gao, M. Wu and X. Yang. p53 Regulates Biosynthesis Through Direct Inactivation of Glucose-6-Phosphate Dehydrogenase. *Nature Cell Biology*, 13:310-316, 2011.

74. X. Hong, R. Song, H. Song, T. Zheng, J. Wang, Y. Liang, S. Qi, Z. Lu, X. Song, H. Jiang, L. Liu and Z. Zhang. PTEN Antagonises Tcl1/hnRNPK-mediated G6PD Pre-mRNA Splicing Which Contributes to Hepatocarcinogenesis. *Gut*, 63:1635-1647, 2014.

75. K. C. Patra and N. Hay. The Pentose Phosphate Pathway and Cancer. *Trends in Biochemical Sciences*, 39:347-354, 2014.

76. K. E. V. H. Christopher K. Mathews, Dean R. Appling, Spencer and J. Anthony-Cahill. *Biochemistry*. Fourth Edition. Pearson Education, New Jersey, 2012.

77. M. Vondrusova, A. Bezawork-Geleta, K. Sachaphibulkij, J. Truksa and J. Neuzil. The Effect of Mitochondrially Targeted Anticancer Agents on Mitochondrial (Super)Complexes. *Methods in Molecular Biology (Clifton, N.J.)*, 1265:195-208, 2015.

78. N. V. Dudkina, R. Kouril, K. Peters, H. P. Braun and E. J. Boekema. Structure and Function of Mitochondrial Supercomplexes. *Biochimica et Biophysica Acta*, 1797:664-670, 2010.

79. R. Vartak, C. A. Porras and Y. Bai. Respiratory Supercomplexes: Structure, Function and Assembly. *Protein Cell*, 4:582-590, 2013.

80. I. Lopez-Fabuel, J. Le Douce, A. Logan, A. M. James, G. Bonvento, M. P. Murphy and A. Almeida. Complex I Assembly Into Supercomplexes Determines Differential Mitochondrial ROS Production in Neurons and Astrocytes. 113:13063-13068, 2016.

81. S. K. N. Marie and S. M. O. Shinjo. Metabolism and Brain Cancer. *Clinics*, 66:33-43, 2011.

82. S. Agnihotri and G. Zadeh. Metabolic Reprogramming in Glioblastoma: the Influence of Cancer Metabolism on Epigenetics and Unanswered Questions. *Neuro-oncology*, 18:160-172, 2016.

83. M. E. Beckner, W. Fellows-Mayle, Z. Zhang, N. R. Agostino, J. A. Kant, B. W. Day and I. F. Pollack. Identification of ATP Citrate Lyase As A Positive Regulator of Glycolytic Function in Glioblastomas. *International Journal of Cancer*, 126:2282-2295, 2010.

84. H. Q. Wang, D. A. Altomare, K. L. Skele, P. I. Poulikakos, F. P. Kuhajda, A. Di Cristofano and J. R. Testa. Positive Feedback Regulation Between AKT Activation and Fatty Acid Synthase Expression in Ovarian Carcinoma Cells. *Oncogene*, 24:3574-3582, 2005.

85. J. A. Menendez and R. Lupu. Fatty Acid Synthase and the lipogenic Phenotype in Cancer Pathogenesis. *Nature Reviews. Cancer*, 7:763-777, 2007.

86. A.-K. Bouzier-Sore and L. Pellerin. Unraveling the Complex Metabolic Nature of Astrocytes. *Frontiers in Cellular Neuroscience*, 7:179, 2013.

87. M. A. Selak, S. M. Armour, E. D. MacKenzie, H. Boulahbel, D. G. Watson, K. D. Mansfield, Y. Pan, M. C. Simon, C. B. Thompson and E. Gottlieb. Succinate Links TCA

Cycle Dysfunction to Oncogenesis by Inhibiting HIF-alpha Prolyl Hydroxylase. *Cancer Cell*, 7:77-85, 2005.

88. N. C. Denko. Hypoxia, HIF1 and Glucose Metabolism in the Solid Tumour. *Nature Reviews. Cancer*, 8:705-713, 2008.

89. W. H. Koppenol, P. L. Bounds and C. V. Dang. Otto Warburg's Contributions to Current Concepts of Cancer Metabolism. *Nature Reviews. Cancer*, 11:325-337, 2011.

90. R. Moreno-Sanchez, A. Marin-Hernandez, E. Saavedra, J. P. Pardo, S. J. Ralph and S. Rodriguez-Enriquez. Who Controls the ATP Supply in Cancer Cells? Biochemistry Lessons to Understand Cancer Energy Metabolism. *The International Journal of Biochemistry Cell Biology*, 50:10-23, 2014.

91. D. F. Wilson, W. L. Rumsey, T. J. Green and J. M. Vanderkooi. The Oxygen Dependence of Mitochondrial Oxidative Phosphorylation Measured by a New Optical Method for Measuring Oxygen Concentration. *The Journal of Biological Chemistry*, 263:2712-2718, 1988.

92. F. Weinberg, R. Hamanaka, W. W. Wheaton, S. Weinberg, J. Joseph, M. Lopez, B. Kalyanaraman, G. M. Mutlu, G. R. Budinger and N. S. Chandel. Mitochondrial Metabolism and ROS Generation Are Essential for Kras-mediated Tumorigenicity. *Proceedings of the National Academy of Sciences of the United States of America*, 107:8788-8793, 2010.

93. P. Gao, I. Tchernyshyov, T. C. Chang, Y. S. Lee, K. Kita, T. Ochi, K. I. Zeller, A. M. De Marzo, J. E. Van Eyk, J. T. Mendell and C. V. Dang. c-Myc Suppression of miR-23a/b Enhances Mitochondrial Glutaminase Expression and Glutamine Metabolism. *Nature*, 458:762-765, 2009.

94. M. Morita, S. P. Gravel, V. Chenard, K. Sikstrom, L. Zheng, T. Alain, V. Gandin, D. Avizonis, M. Arguello, C. Zakaria, S. McLaughlan, Y. Nouet, A. Pause, M. Pollak, E. Gottlieb, O. Larsson, J. St-Pierre, I. Topisirovic and N. Sonenberg. mTORC1 Controls

Mitochondrial Activity and Biogenesis Through 4E-BP-dependent Translational Regulation. *Cell Metabolism*, 18:698-711, 2013.

95. M. Janiszewska, M. L. Suva, N. Riggi, R. H. Houtkooper, J. Auwerx, V. Clement-Schatlo, I. Radovanovic, E. Rheinbay, P. Provero and I. Stamenkovic. Imp2 Controls Oxidative Phosphorylation and is Crucial for Preserving Glioblastoma Cancer Stem Cells. *Genes Development*, 26:1926-1944, 2012.

96. A. Roesch, A. Vultur, I. Bogeski, H. Wang, K. M. Zimmermann, D. Speicher, C. Korbel, M. W. Laschke, P. A. Gimotty, S. E. Philipp, E. Krause, S. Patzold, J. Villanueva, C. Krepler, M. Fukunaga-Kalabis, M. Hoth, B. C. Bastian, T. Vogt and M. Herlyn. Overcoming Intrinsic Multidrug Resistance in Melanoma by Blocking the Mitochondrial Respiratory Chain of Slow-cycling JARID1B(high) Cells. *Cancer Cell*, 23:811-825, 2013.

97. V. S. LeBleu, J. T. O'Connell, K. N. Gonzalez Herrera, H. Wikman, K. Pantel, M. C. Haigis, F. M. de Carvalho, A. Damascena, L. T. Domingos Chinen, R. M. Rocha, J. M. Asara and R. Kalluri. PGC-1alpha Mediates Mitochondrial Biogenesis and Oxidative Phosphorylation in Cancer Cells to Promote Metastasis. *Nature Cell Biology*, 16:992-1003, 1001-1015, 2014.

98. Y. C. Chae, A. Angelin, S. Lisanti, A. V. Kossenkov, K. D. Speicher, H. Wang, J. F. Powers, A. S. Tischler, K. Pacak, S. Fliedner, R. D. Michalek, E. D. Karoly, D. C. Wallace, L. R. Languino, D. W. Speicher and D. C. Altieri. Landscape of the Mitochondrial Hsp90 Metabolome in Tumours. *Nature Communications*, 4:2139, 2013.

99. A. Cole, Z. Wang, E. Coyaud, V. Voisin, M. Gronda, Y. Jitkova, R. Mattson, R. Hurren, S. Babovic, N. Maclean, I. Restall, X. Wang, D. V. Jeyaraju, M. A. Sukhai, S. Prabha, S. Bashir, A. Ramakrishnan, E. Leung, Y. H. Qia, N. Zhang, K. R. Combes, T. Ketela, F. Lin, W. A. Houry, A. Aman, R. Al-Awar, W. Zheng, E. Wienholds, C. J. Xu, J. Dick, J. C. Wang, J. Moffat, M. D. Minden, C. J. Eaves, G. D. Bader, Z. Hao, S. M. Kornblau, B. Raught and A. D. Schimmer. Inhibition of the Mitochondrial Protease ClpP as a Therapeutic Strategy for Human Acute Myeloid Leukemia. *Cancer Cell*, 27:864-876, 2015.

100. M. C. Caino and D. C. Altieri. Molecular Pathways: Mitochondrial Reprogramming in Tumor Progression and Therapy. *Clinical Cancer Research : An Official Journal of the American Association for Cancer Research*, 22:540-545, 2016.

101. E. Currie, A. Schulze, R. Zechner, T. C. Walther and R. V. Farese, Jr. Cellular Fatty Acid Metabolism and Cancer. *Cell Metabolism*, 18:153-161, 2013.

102. R. J. DeBerardinis, A. Mancuso, E. Daikhin, I. Nissim, M. Yudkoff, S. Wehrli and C. B. Thompson. Beyond Aerobic Glycolysis: Transformed Cells Can Engage in Glutamine Metabolism that Exceeds the Requirement for Protein and Nucleotide Synthesis. *Proceedings of the National Academy of Sciences of the United States of America*, 104:19345-19350, 2007.

103. C. V. Dang, A. Le and P. Gao. MYC-induced Cancer Cell Energy Metabolism and Therapeutic Opportunities. *Clinical Cancer Research : An Official Journal of the American Association for Cancer Research*, 15:6479-6483, 2009.

104. W. Lu, H. Pelicano and P. Huang. Cancer Metabolism: is Glutamine Sweeter Than Glucose? *Cancer Cell*, 18:199-200, 2010.

105. M. Younes, L. V. Lechago, J. R. Somoano, M. Mosharaf and J. Lechago. Wide Expression of the Human Erythrocyte Glucose Transporter Glut1 in Human Cancers. *Cancer Research*, 56:1164-1167, 1996.

106. T. N. Seyfried, R. Flores, A. M. Poff, D. P. D'Agostino and P. Mukherjee. Metabolic Therapy: A New Paradigm for Managing Malignant Brain Cancer. *Cancer Letters*, 356:289-300, 2015.

107. Z. C. Ye and H. Sontheimer. Glioma Cells Release Excitotoxic Concentrations of Glutamate. *Cancer Research*, 59:4383-4391, 1999.

108. M. Yuneva. Finding an "Achilles' heel" of Cancer: the Role of Glucose and Glutamine Metabolism in the Survival of Transformed Cells. *Cell Cycle*, 7:2083-2089, 2008.

109. S. A. van Lith, A. C. Navis, K. Verrijp, S. P. Niclou, R. Bjerkvig, P. Wesseling, B. Tops, R. Molenaar, C. J. van Noorden and W. P. Leenders. Glutamate as Chemotactic Fuel for Diffuse Glioma Cells: Are They Glutamate Suckers? *Biochimica et Biophysica Acta*, 1846:66-74, 2014.

110. M. Fredericks and R. B. Ramsey. 3-Oxo Acid Coenzyme A Transferase Activity in Brain and Tumors of the Nervous System. *Journal of Neurochemistry*, 31:1529-1531, 1978.

111. G. D. Maurer, D. P. Brucker, O. Bahr, P. N. Harter, E. Hattingen, S. Walenta, W. Mueller-Klieser, J. P. Steinbach and J. Rieger. Differential Utilization of Ketone Bodies by Neurons and Glioma Cell Lines: A Rationale for Ketogenic Diet as Experimental Glioma Therapy. *BMC Cancer*, 11:315, 2011.

112. A. M. Poff, C. Ari, P. Arnold, T. N. Seyfried and D. P. D'Agostino. Ketone Supplementation Decreases Tumor Cell Viability and Prolongs Survival of Mice with Metastatic Cancer. *International Journal of Cancer*, 135:1711-1720, 2014.

113. Z. C. Ye, J. D. Rothstein and H. Sontheimer. Compromised Glutamate Transport in Human Glioma Cells: Reduction-mislocalization of Sodium-Dependent Glutamate Transporters and Enhanced Activity of Cystine-Glutamate Exchange. *The Journal of Neuroscience : the Official Journal of the Society for Neuroscience*, 19:10767-10777, 1999.

114. U. E. Martinez-Outschoorn, M. Peiris-Pages, R. G. Pestell, F. Sotgia and M. P. Lisanti. Cancer Metabolism: A Therapeutic Perspective. *Nature Reviews. Clinical Oncology*, 2016.

115. B. C. Liang and M. Grootveld. The Importance of Mitochondria in the Tumourigenic Phenotype: Gliomas as the Paradigm. *International Journal of Molecular Medicine*, 27:159-171, 2011.

116. C. E. Griguer and C. R. Oliva. Bioenergetics Pathways and Therapeutic Resistance in Gliomas: Emerging Role of Mitochondria. *Current Pharmaceutical Design*, 17:2421-2427, 2011.

117. F. M. Santandreu, M. Brell, A. H. Gene, R. Guevara, J. Oliver, M. E. Couce and P. Roca. Differences in Mitochondrial Function and Antioxidant Systems Between Regions of Human Glioma. *Cellular Physiology and Biochemistry : International Journal of Experimental Cellular Physiology, Biochemistry, and Pharmacology*, 22:757-768, 2008.

118. G. J. Arismendi-Morillo and A. V. Castellano-Ramirez. Ultrastructural Mitochondrial Pathology in Human Astrocytic Tumors: Potentials Implications Pro-Therapeutics Strategies. *Journal of Electron Microscopy*, 57:33-39, 2008.

119. G. Arismendi-Morillo. Electron Microscopy Morphology of the Mitochondrial Network in Gliomas and Their Vascular Microenvironment. *Biochimica et Biophysica Acta*, 1807:602-608, 2011.

120. R. L. Correia, S. M. Oba-Shinjo, M. Uno, N. Huang and S. K. Marie. Mitochondrial DNA Depletion and Its Correlation with TFAM, TFB1M, TFB2M and POLG in Human Diffusely Infiltrating Astrocytomas. *Mitochondrion*, 11:48-53, 2011.

121. R. J. DeBerardinis, J. J. Lum, G. Hatzivassiliou and C. B. Thompson. The Biology of Cancer: Metabolic Reprogramming Fuels Cell Growth and Proliferation. *Cell Metabolism*, 7:11-20, 2008.

122. D. W. Parsons, S. Jones, X. Zhang, J. C. Lin, R. J. Leary, P. Angenendt, P. Mankoo, H. Carter, I. M. Siu, G. L. Gallia, A. Olivi, R. McLendon, B. A. Rasheed, S. Keir, T. Nikolskaya, Y. Nikolsky, D. A. Busam, H. Tekleab, L. A. Diaz, Jr., J. Hartigan, D. R. Smith, R. L. Strausberg, S. K. Marie, S. M. Shinjo, H. Yan, G. J. Riggins, D. D. Bigner, R.

Karchin, N. Papadopoulos, G. Parmigiani, B. Vogelstein, V. E. Velculescu and K. W. Kinzler. An Integrated Genomic Analysis of Human Glioblastoma Multiforme. *Science (New York, N.Y.)*, 321:1807-1812, 2008.

123. R. A. Cairns, I. S. Harris and T. W. Mak. Regulation of Cancer Cell Metabolism. *Nature Reviews. Cancer*, 11:85-95, 2011.

124. B. E. Baysal, R. E. Ferrell, J. E. Willett-Brozick, E. C. Lawrence, D. Myssiorek, A. Bosch, A. van der Mey, P. E. Taschner, W. S. Rubinstein, E. N. Myers, C. W. Richard, 3rd, C. J. Cornelisse, P. Devilee and B. Devlin. Mutations in SDHD, a Mitochondrial Complex II Gene, in Hereditary Paraganglioma. *Science (New York, N.Y.)*, 287:848-851, 2000.

125. B. N. Finck and D. P. Kelly. PGC-1 Coactivators: Inducible Regulators of Energy Metabolism in Health and Disease. *The Journal of Clinical Investigation*, 116:615-622, 2006.

126. C. Handschin and B. M. Spiegelman. The Role of Exercise and PGC1alpha in Inflammation and Chronic Disease. *Nature*, 454:463-469, 2008.

127. C. Liu and J. D. Lin. PGC-1 Coactivators in the Control of Energy Metabolism. *Acta Biochimica et Biophysica Sinica*, 43:248-257, 2011.

128. M. E. Patti, A. J. Butte, S. Crunkhorn, K. Cusi, R. Berria, S. Kashyap, Y. Miyazaki, I. Kohane, M. Costello, R. Saccone, E. J. Landaker, A. B. Goldfine, E. Mun, R. DeFronzo, J. Finlayson, C. R. Kahn and L. J. Mandarino. Coordinated Reduction of Genes of Oxidative Metabolism in Humans with Insulin Resistance and Diabetes: Potential Role of PGC1 and NRF1. *Proceedings of the National Academy of Sciences of the United States of America*, 100:8466-8471, 2003.

129. V. K. Mootha, C. Handschin, D. Arlow, X. Xie, J. St Pierre, S. Sihag, W. Yang, D. Altshuler, P. Puigserver, N. Patterson, P. J. Willy, I. G. Schulman, R. A. Heyman, E. S. Lander and B. M. Spiegelman. Erralpha and Gabpa/b Specify PGC-1alpha-dependent

Oxidative Phosphorylation Gene Expression that is Altered in Diabetic Muscle. *Proceedings of the National Academy of Sciences of the United States of America*, 101:6570-6575, 2004.

130. G. Haemmerle, T. Moustafa, G. Woelkart, S. Buttner, A. Schmidt, T. van de Weijer, M. Hesselink, D. Jaeger, P. C. Kienesberger, K. Zierler, R. Schreiber, T. Eichmann, D. Kolb, P. Kotzbeck, M. Schweiger, M. Kumari, S. Eder, G. Schoiswohl, N. Wongsiriroj, N. M. Pollak, F. P. Radner, K. Preiss-Landl, T. Kolbe, T. Rulicke, B. Pieske, M. Trauner, A. Lass, R. Zimmermann, G. Hoefler, S. Cinti, E. E. Kershaw, P. Schrauwen, F. Madeo, B. Mayer and R. Zechner. ATGL-mediated Fat Catabolism Regulates Cardiac Mitochondrial Function via PPAR-alpha and PGC-1. *Nature Medicine*, 17:1076-1085, 2011.

131. S. A. Khan, A. Sathyanarayan, M. T. Mashek, K. T. Ong, E. E. Wollaston-Hayden and D. G. Mashek. ATGL-catalyzed Lipolysis Regulates SIRT1 to Control PGC-1alpha/PPAR-alpha Signaling. *Diabetes*, 64:418-426, 2015.

132. A. R. La Spada. PPARGC1A/PGC-1α, TFEB and Enhanced Proteostasis in Huntington Disease: Defining Regulatory Linkages Between Energy Production and Protein Organelle Quality Control. *Autophagy*, 8:1845-1847, 2012.

133. D. Knutti, D. Kressler and A. Kralli. Regulation of the Transcriptional Coactivator PGC-1 via MAPK-sensitive Interaction With a Repressor. *Proceedings of the National Academy of Sciences of the United States of America*, 98:9713-9718, 2001.

134. X. Li, B. Monks, Q. Ge and M. J. Birnbaum. Akt/PKB Regulates Hepatic Metabolism by Directly Inhibiting PGC-1alpha Transcription Coactivator. *Nature*, 447:1012-1016, 2007.

135. M. M. Rytinki and J. J. Palvimo. SUMOylation Attenuates the Function of PGC-1alpha. *The Journal of Biological Chemistry*, 284:26184-26193, 2009.

136. K. Bhalla, B. J. Hwang, R. E. Dewi, L. Ou, W. Twaddel, H. B. Fang, S. B. Vafai, F. Vazquez, P. Puigserver, L. Boros and G. D. Girnun. PGC1alpha Promotes Tumor Growth

by Inducing Gene Expression Programs Supporting Lipogenesis. *Cancer Research*, 71:6888-6898, 2011.

137. Z. Tan, X. Luo, L. Xiao, M. Tang, A. M. Bode, Z. Dong and Y. Cao. The Role of PGC1alpha in Cancer Metabolism and Its Therapeutic Implications. *Molecular Cancer Therapeutics*, 15:774-782, 2016.

138. D. Krell, M. Assoku, M. Galloway, P. Mulholland, I. Tomlinson and C. Bardella. Screen for IDH1, IDH2, IDH3, D2HGDH and L2HGDH Mutations in Glioblastoma. *PloS One*, 6:19868, 2011.

139. V. Gogvadze and B. Zhivotovsky. Alteration of Mitochondrial Function and Cell Sensitization to Death. *Journal of Bioenergetics and Biomembranes*, 39:23-30, 2007.

140. W. Yu, K. E. Dittenhafer-Reed and J. M. Denu. SIRT3 Protein Deacetylates Isocitrate Dehydrogenase 2 (IDH2) and Regulates Mitochondrial Redox Status. *The Journal of Biological Chemistry*, 287:14078-14086, 2012.

141. J. Balss, J. Meyer, W. Mueller, A. Korshunov, C. Hartmann and A. von Deimling. Analysis of the IDH1 Codon 132 Mutation in Brain Tumors. *Acta Neuropathologica*, 116:597-602, 2008.

142. H. Yan, D. W. Parsons, G. Jin, R. McLendon, B. A. Rasheed, W. Yuan, I. Kos, I. Batinic-Haberle, S. Jones, G. J. Riggins, H. Friedman, A. Friedman, D. Reardon, J. Herndon, K. W. Kinzler, V. E. Velculescu, B. Vogelstein and D. D. Bigner. IDH1 and IDH2 Mutations in Gliomas. *The New England Journal of Medicine*, 360:765-773, 2009.

143. C. Hartmann, J. Meyer, J. Balss, D. Capper, W. Mueller, A. Christians, J. Felsberg, M. Wolter, C. Mawrin, W. Wick, M. Weller, C. Herold-Mende, A. Unterberg, J. W. Jeuken, P. Wesseling, G. Reifenberger and A. von Deimling. Type and Frequency of IDH1 and IDH2 Mutations are Related to Astrocytic and Oligodendroglial Differentiation and Age: A Study of 1,010 Diffuse Gliomas. *Acta Neuropathologica*, 118:469-474, 2009.

144. N. K. Kloosterhof, L. B. Bralten, H. J. Dubbink, P. J. French and M. J. van den Bent. Isocitrate Dehydrogenase-1 Mutations: A Fundamentally New Understanding of Diffuse Glioma? *The Lancet Oncology*, 12:83-91, 2011.

145. R. Leonardi, C. Subramanian, S. Jackowski and C. O. Rock. Cancer-associated Isocitrate Dehydrogenase Mutations Inactivate NADPH-Dependent Reductive Carboxylation. *The Journal of Biological Chemistry*, 287:14615-14620, 2012.

146. P. S. Ward, J. Patel, D. R. Wise, O. Abdel-Wahab, B. D. Bennett, H. A. Coller, J. R. Cross, V. R. Fantin, C. V. Hedvat, A. E. Perl, J. D. Rabinowitz, M. Carroll, S. M. Su, K. A. Sharp, R. L. Levine and C. B. Thompson. The Common Feature of Leukemia-Associated IDH1 and IDH2 Mutations is a Neomorphic Enzyme Activity Converting Alpha-Ketoglutarate to 2-hydroxyglutarate. *Cancer Cell*, 17:225-234, 2010.

147. S. Zhao, Y. Lin, W. Xu, W. Jiang, Z. Zha, P. Wang, W. Yu, Z. Li, L. Gong, Y. Peng, J. Ding, Q. Lei, K. L. Guan and Y. Xiong. Glioma-derived Mutations in IDH1 Dominantly Inhibit IDH1 Catalytic Activity and Induce HIF-1alpha. *Science (New York, N.Y.)*, 324:261-265, 2009.

148. Z. J. Reitman, C. G. Duncan, E. Poteet, A. Winters, L. J. Yan, D. M. Gooden, I. Spasojevic, L. G. Boros, S. H. Yang and H. Yan. Cancer-associated Isocitrate Dehydrogenase 1 (IDH1) R132H Mutation and d-2-hydroxyglutarate Stimulate Glutamine Metabolism Under Hypoxia. *The Journal of Biological Chemistry*, 289:23318-23328, 2014.

149. J. A. Losman and W. G. Kaelin, Jr. What a Difference a Hydroxyl Makes: Mutant IDH, (R)-2-hydroxyglutarate, and Cancer. *Genes and Development*, 27:836-852, 2013.

150. D. Hanahan and R. A. Weinberg. Hallmarks of Cancer: The Next Generation. *Cell*, 144:646-674, 2011.

151. O. Warburg. On the Origin of Cancer Cells. *Science (New York, N.Y.)*, 123:309-314, 1956.

152. O. Warburg. On Respiratory Impairment in Cancer Cells. *Science (New York, N.Y.)*, 124:269-270, 1956.

153. S. Y. Lunt and M. G. Vander Heiden. Aerobic Glycolysis: Meeting The Metabolic Requirements of Cell Proliferation. *Annual Review of Cell and Developmental Biology*, 27:441-464, 2011.

154. M. G. Vander Heiden, L. C. Cantley and C. B. Thompson. Understanding The Warburg Effect: The Metabolic Requirements of Cell Proliferation. *Science (New York, N.Y.)*, 324:1029-1033, 2009.

155. P. Gao, L. Sun, X. He, Y. Cao and H. Zhang. MicroRNAs and the Warburg Effect: New Players in an Old Arena. *Current Gene Therapy*, 12:285-291, 2012.

156. J. W. Kim, K. I. Zeller, Y. Wang, A. G. Jegga, B. J. Aronow, K. A. O'Donnell and C. V. Dang. Evaluation of myc E-box Phylogenetic Footprints in Glycolytic Genes by Chromatin Immunoprecipitation Assays. *Molecular and Cellular Biology*, 24:5923-5936, 2004.

157. T. Mikawa, L. L. ME, A. Takaori-Kondo, N. Inagaki, M. Yokode and H. Kondoh. Dysregulated Glycolysis as an Oncogenic Event. *Cellular and Molecular Life Sciences : CMLS*, 72:1881-1892, 2015.

158. D. Huang, C. Li and H. Zhang. Hypoxia and Cancer Cell Metabolism. *Acta Biochimica et Biophysica Sinica*, 46:214-219, 2014.

159. C. Zhang, J. Liu, R. Wu, Y. Liang, M. Lin, J. Liu, C. S. Chan, W. Hu and Z. Feng. Tumor Suppressor p53 Negatively Regulates Glycolysis Stimulated by Hypoxia Through Its Target RRAD. *Oncotarget*, 5:5535-5546, 2014.

160. R. Moreno-Sanchez, S. Rodriguez-Enriquez, A. Marin-Hernandez and E. Saavedra. Energy Metabolism in Tumor Cells. *The FEBS Journal*, 274:1393-1418, 2007.

161. M. Guppy, P. Leedman, X. Zu and V. Russell. Contribution by Different Fuels and Metabolic Pathways to The Total ATP Turnover of Proliferating MCF-7 Breast Cancer Cells. *The Biochemical Journal*, 364:309-315, 2002.

162. M. Martin, B. Beauvoit, P. J. Voisin, P. Canioni, B. Guerin and M. Rigoulet. Energetic and Morphological Plasticity of C6 Glioma Cells Grown on 3-D Support; Effect of Transient Glutamine Deprivation. *Journal of Bioenergetics And Biomembranes*, 30:565-578, 1998.

163. P. Pasdois, C. Deveaud, P. Voisin, V. Bouchaud, M. Rigoulet and B. Beauvoit. Contribution of the Phosphorylable Complex I in The Growth Phase-Dependent Respiration of C6 Glioma Cells *in vitro*. *Journal of Bioenergetics and Biomembranes*, 35:439-450, 2003.

164. R. B. Hamanaka and N. S. Chandel. Targeting Glucose Metabolism for Cancer Therapy. *The Journal of Experimental Medicine*, 209:211-215, 2012.

165. R. J. Deberardinis, N. Sayed, D. Ditsworth and C. B. Thompson. Brick by Brick: Metabolism and Tumor Cell Growth. *Current Opinion in Genetics and Development*, 18:54-61, 2008.

166. S. Ganapathy-Kanniappan, J. F. Geschwind, R. Kunjithapatham, M. Buijs, J. A. Vossen, I. Tchernyshyov, R. N. Cole, L. H. Syed, P. P. Rao, S. Ota and M. Vali. Glyceraldehyde-3-phosphate Dehydrogenase (GAPDH) is Pyruvylated During 3-bromopyruvate Mediated Cancer Cell Death. *Anticancer Research*, 29:4909-4918, 2009.

167. S. Ganapathy-Kanniappan, R. Kunjithapatham and J. F. Geschwind. Glyceraldehyde-3-phosphate Dehydrogenase: A Promising Target for Molecular Therapy in Hepatocellular Carcinoma. *Oncotarget*, 3:940-953, 2012.

168. S. Ganapathy-Kanniappan, R. Kunjithapatham and J. F. Geschwind. Anticancer Efficacy of The Metabolic Blocker 3-Bromopyruvate: Specific Molecular Targeting. *Anticancer Research*, 33:13-20, 2013.

169. L. J. Savic, J. Chapiro, G. Duwe and J. F. Geschwind. Targeting Glucose Metabolism in Cancer: New Class of Agents for Loco-Regional and Systemic Therapy of Liver Cancer and Beyond? *Hepatic Oncology*, 3:19-28, 2016.

170. B. Dwarakanath and V. Jain. Targeting Glucose Metabolism with 2-deoxy-D-glucose for Improving Cancer Therapy. *Future Oncology (London, England)*, 5:581-585, 2009.

171. J. C. Maher, A. Krishan and T. J. Lampidis. Greater Cell Cycle Inhibition and Cytotoxicity Induced by 2-deoxy-D-glucose in Tumor Cells Treated Under Hypoxic vs Aerobic Conditions. *Cancer Chemotherapy and Pharmacology*, 53:116-122, 2004.

172. D. Zhang, J. Li, F. Wang, J. Hu, S. Wang and Y. Sun. 2-Deoxy-D-glucose Targeting of Glucose Metabolism in Cancer Cells as a Potential Therapy. *Cancer Letters*, 355:176-183, 2014.

173. Z. H. Zhou, D. B. McCarthy, C. M. O'Connor, L. J. Reed and J. K. Stoops. The Remarkable Structural and Functional Organization of The Eukaryotic Pyruvate Dehydrogenase Complexes. *Proceedings of the National Academy of Sciences of the United States of America*, 98:14802-14807, 2001.

174. M. Smolle, A. E. Prior, A. E. Brown, A. Cooper, O. Byron and J. G. Lindsay. A New Level of Architectural Complexity in The Human Pyruvate Dehydrogenase Complex. *The Journal of Biological Chemistry*, 281:19772-19780, 2006.

175. C. A. Brautigam, R. M. Wynn, J. L. Chuang, M. Machius, D. R. Tomchick and D. T. Chuang. Structural Insight into Interactions Between Dihydrolipoamide Dehydrogenase E3 and E3 Binding Protein of Human Pyruvate Dehydrogenase Complex. *Structure*, 14:611-621, 2006.

176. M. M. Bowker-Kinley, W. I. Davis, P. Wu, R. A. Harris and K. M. Popov. Evidence for Existence of Tissue-Specific Regulation Of The Mammalian Pyruvate Dehydrogenase Complex. *The Biochemical Journal*, 329:191-196, 1998.

177. O. B. Evans and P. W. Stacpoole. Prolonged Hypolactatemia and Increased Total Pyruvate Dehydrogenase Activity by Dichloroacetate. *Biochemical Pharmacology*, 31:1295-1300, 1982.

178. T. E. Roche, J. C. Baker, X. Yan, Y. Hiromasa, X. Gong, T. Peng, J. Dong, A. Turkan and S. A. Kasten. Distinct Regulatory Properties of Pyruvate Dehydrogenase Kinase and Phosphatase Isoforms. *Progress in Nucleic Acid Research and Molecular Biology*, 70:33-75, 2001.

179. S. Kankotia and P. W. Stacpoole. Dichloroacetate and Cancer: New Home for an Orphan Drug? *Biochimica et Biophysica Acta*, 1846:617-629, 2014.

180. P. W. Stacpoole. The Dichloroacetate Dilemma: Environmental Hazard Versus Therapeutic Goldmine Both or Neither? *Environmental Health Perspectives*, 119:155-158, 2011.

181. P. W. Stacpoole. The Pharmacology of Dichloroacetate. *Metabolism: Clinical and Experimental*, 38:1124-1144, 1989.

182. R. Zhang, T. L. Tremblay, A. McDermid, P. Thibault and D. Stanimirovic. Identification of Differentially Expressed Proteins in Human Glioblastoma Cell Lines and Tumors. *Glia*, 42:194-208, 2003.

183. J. Kalinina, J. Peng, J. C. Ritchie and E. G. Van Meir. Proteomics of Gliomas: Initial Biomarker Discovery and Evolution Of Technology. *Neuro-oncology*, 13:926-942, 2011.

184. J. R. Yates, 3rd. The Revolution and Evolution of Shotgun Proteomics for Large-Scale Proteome Analysis. *Journal of the American Chemical Society*, 135:1629-1640, 2013.

185. R. Aebersold and M. Mann. Mass Spectrometry-Based Proteomics. *Nature*, 422:198-207, 2003.

186. B. Domon and R. Aebersold. Mass Spectrometry and Protein Analysis. *Science (New York, N.Y.)*, 312:212-217, 2006.

187. W. Zhou, L. A. Liotta and E. F. Petricoin. Cancer Metabolism and Mass Spectrometry-Based Proteomics. *Cancer Letters*, 356:176-183, 2015.

188. R. Matthiesen and J. Bunkenborg. Introduction to Mass Spectrometry-Based Proteomics. *Methods in Molecular Biology*, 1007:1-45, 2013.

189. S. E. Ong and M. Mann. Mass Spectrometry-Based Proteomics Turns Quantitative. *Nature Chemical Biology*, 1:252-262, 2005.

190. Y. Zhang, B. R. Fonslow, B. Shan, M. C. Baek and J. R. Yates, 3rd. Protein Analysis by Shotgun/Bottom-Up Proteomics. *Chemical Reviews*, 113:2343-2394, 2013.

191. B. Domon and R. Aebersold. Options and Considerations When Selecting a Quantitative Proteomics Strategy. *Nature Biotechnology*, 28:710-721, 2010.

192. E. I. Chen and J. R. Yates, 3rd. Cancer Proteomics by Quantitative Shotgun Proteomics. *Molecular Oncology*, 1:144-159, 2007.

193. W. X. Schulze and B. Usadel. Quantitation in Mass-Spectrometry-Based Proteomics. *Annual Review of Plant Biology*, 61:491-516, 2010.

194. L. McHugh and J. W. Arthur. Computational Methods for Protein Identification from Mass Spectrometry Data. *PLOS Computational Biology*, 4:12, 2008.

195. X. Han, A. Aslanian and J. R. Yates, 3rd. Mass Spectrometry for Proteomics. *Current Opinion in Chemical Biology*, 12:483-490, 2008.

196. R. E. Lloyd, K. Keatley, D. T. Littlewood, B. Meunier, W. V. Holt, Q. An, S. C. Higgins, S. Polyzoidis, K. F. Stephenson, K. Ashkan, H. L. Fillmore, G. J. Pilkington and

J. E. McGeehan. Identification and Functional Prediction of Mitochondrial Complex III and IV Mutations Associated with Glioblastoma. *Neuro-oncology*, 17:942-952, 2015.

197. C. E. Griguer, C. R. Oliva and G. Y. Gillespie. Glucose Metabolism Heterogeneity in Human and Mouse Malignant Glioma Cell Lines. *Journal of Neuro-Oncology*, 74:123-133, 2005.

198. M. L. Goodwin, L. B. Gladden, M. W. N. Nijsten and K. B. Jones. Lactate and Cancer: Revisiting the Warburg Effect in an Era of Lactate Shuttling. *Frontiers in Nutrition*, 1:27, 2014.

199. J. Li, S. Zhu, J. Tong, H. Hao, J. Yang, Z. Liu and Y. Wang. Suppression of lactate dehydrogenase A Compromises Tumor Progression by Downregulation of the Warburg Effect in Glioblastoma. *Neuroreport*, 27:110-115, 2016.

200. L. B. Sullivan and N. S. Chandel. Mitochondrial Reactive Oxygen Species and Cancer. *Cancer and Metabolism*, 2:17, 2014.